

**COMMERCIAL FOREST SPECIES DISCRIMINATION AND MAPPING USING  
IMAGE TEXTURE COMPUTED FROM WORLDVIEW-2 PAN SHARPENED  
IMAGERY IN KWAZULU-NATAL, SOUTH AFRICA**

**Bongokuhle S’phesihle Sibiya**

**215035638**

Thesis submitted to the college of Agriculture, Engineering and Science, at the University  
of Kwazulu-Natal, in fulfilment of the academic requirements of the degree of Master of  
Science in Geography and Environmental Science

(Specialization: GIS and Remote Sensing)

Pietermaritzburg South

Africa

## Abstract

Forest species discrimination is vital for precise and dependable information, essential for commercial forest management and monitoring. Recently, the adoption of remote sensing approaches has become an important source of information in commercial forest management. However, previous studies have utilized spectral data or vegetation indices to detect and map commercial forest species, with less focus on the spatial elements. Therefore, this study using image texture aims to discriminate commercial forest plantations (i.e. *A. mearnsii*, *E. dunnii*, *E. grandis* and *P. patula*) computed from a 0.5m WorldView-2 pan-sharpened image in KwaZuluNatal, South Africa. The first objective of the study was to discriminate commercial forest species using image texture computed from a 0.5m WorldView-2 pan-sharpened image and the Partial Least Squares Discriminate Analysis (PLS-DA) algorithm. The results indicated that the image texture model (overall accuracy (OA) = 77%, kappa = 0.69) outperformed both the vegetation indices model (OA = 69%, kappa = 0.59) and raw spectral bands model (OA = 64%, kappa = 0.52). The most successful texture parameters selected by PLS-DA were mean, correlation, and homogeneity, which were primarily computed from the red-edge, NIR1 and NIR2 bands. Lastly, the 7x7 moving window was commonly selected by the PLS-DA model when compared to the 3x3 and 5x5 moving windows. The second objective of the study was to explore the utility of texture combinations computed from a fused 0.5m WorldView-2 image in discriminating commercial forest species in conjunction with the PLS-DA and Sparse Partial Least Squares Discriminate Analysis (SPLS-DA) algorithm. The accuracies achieved using SPLS-DA model, which performed variable selection and dimension reduction simultaneously yielded an overall accuracy of 86%. In contrast, the PLS-DA and variable importance in the projection (VIP) produced an overall classification accuracy of 81%. Generally, the finding of this study demonstrated the ability of image texture to precisely provide adequate information that is essential for tree species mapping and monitoring.

**Keywords:** Forest species discrimination, image-texture, texture combinations, PLS-DA, SPLSDA, WorldView-2 pan-sharpened imagery.

### **Preface**

This study was conducted in the School of Agricultural, Earth and Environmental Sciences, University of KwaZulu-Natal, Pietermaritzburg, South Africa, under the supervision of Dr. Romano Lottering, Prof John Odindi.

I declare that the work presented in this thesis has never been submitted in any form to any other institution. This work represents my original work except where due acknowledgements are made.

Bongokuhle S’phesihle Sibiya Signed:



Date: 01/09/2021

As the candidate’s supervisor, I certify the aforementioned statement and have approved this thesis for submission.

Dr. Romano Lottering

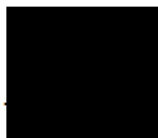
Signed



. Date...22/11/2021

Prof John Odindi

Signed...



Date...24/11/2021

### **Declaration**

I Bongokuhle S'phesihle Sibiya, declare that:

1. The research reported in this thesis, except where otherwise indicated is my original research.
2. This thesis has not been submitted for any degree or examination at any other institution.
3. This thesis does not contain other person's data, pictures, graphs, or other information, unless specifically acknowledged as being sourced from other persons.
4. This thesis does not contain other persons writing, unless specifically acknowledged as being sourced from other researchers. Where other written sources have been quoted:
  - a. Their words have been re-written, and the general information attributed to them has been referenced.
  - b. Where their exact words have been used, their writing has been placed in italics inside quotation marks and referenced
5. This thesis does not contain text, graphics or tables copied and pasted from the internet, unless specifically acknowledged, and the source being detailed in the thesis and in the references section.

Signed: \_\_\_\_\_



Date: 01/09/2021

## **Declaration – Publications**

**Publication 1:** Bongokuhle Sibiya, Romano Lottering & John Odindi, 2021. Discriminating commercial forest species using image texture computed from a WorldView-2 pan-sharpened image and partial least squares discriminant analysis. *Remote Sensing Applications: Society and Environment*, p.100605.

**Publication 2:** Bongokuhle Sibiya, Romano Lottering & John Odindi, 2021. Utility of texture combinations computed from fused WorldView-2 imagery in discriminating commercial Forest species, *Geocarto International*, DOI: [10.1080/10106049.2021.1952316](https://doi.org/10.1080/10106049.2021.1952316)

The work was done by the first author under the guidance and supervision of the second and third authors.

School of Agricultural, Earth and Environmental Sciences, College of Agriculture, Engineering and Science, University of KwaZulu-Natal, Pietermaritzburg, Private Bag X01, Scottsville, 3209, South Africa.

### **Dedication**

This dissertation is dedicated to my beloved family, for believing, trusting, and granting me the opportunity to further my education. I want to continue making you proud.

## Acknowledgement

**You make all things work together for my Good! You once came to Moses and said, “I’m Jehovah, nothing is too hard for me”!** Therefore, I would first and foremost like to thank God, **Honour and Glory belongs to you Lord Jesus!** Without his blessings, direction, and unconditional love, none of this would have been possible.

I would also like to express my gratitude to the School of Agricultural, Earth and Environmental Sciences and the Geography Department University of KwaZulu-Natal, for granting me an opportunity to pursue my Masters, **Thank you.** To my supervisor Doctor Romano Lottering, who spent day and night to ensure that this project smoothly sailed on till today, also for his constructive scientific criticism, patience and commitment in guiding this work, and most importantly for extending his professional expertise and knowledge towards the success of this research, **Huge Thanks.** Thanks to Professor John Odindi (my co-supervisor), for his commitment and passion to see this work progresses, especially his advices and expertise from the beginning and completion of this study.

I would also give special thanks to my friends and colleagues, Sizwe Hlatshwayo, Trylee Matongera, Dr Shenelle Lottering, Lwando Royimani, Mrs Shanita Ramroop, Thembinkosi Mcunu, Dr L.S Chetty, Thanda Khumalo, Nana Khomo, Manene Singata, Mthembeni Mngadi, Msawenkosi Dlamini, Raymond Mtolo, Mxolisi Protas Dlamini, Phindile Mthembu, Nkanyiso Zungu, Menzi Mbense, Bright Ntethe, Sibalukhulu (KZNDOE), Tsitsi Dube, Anele Mthembu, Nokwa Xaba. I thank Nwabisa Mkhize, Samuel Kumbula and Isreal Odebili for proof reading and strengthening this work.

I also want to acknowledge the support, prayers and love I received from the Gospel of Jesus Christ Ministries (JCM) at Panorama. Thank you for teaching me to be humble in times of success and above all thank you for your encouragement and taking care of my spiritual needs. To Siyanda Ngcongo, Khanyisani Dladla and Xolisile Khanyile, thank you for accommodating me. I am greatly indebted to my family for their incessant prayers. **Mom you are the greatest!**

## Table of Contents

Abstract.....	ii
Preface .....	iii
Declaration.....	iv
Declaration – Publications .....	v
Dedication.....	vi
Acknowledgement .....	vii
List of Figures.....	xi
List of Tables .....	xii
CHAPTER ONE.....	1
1. GENERAL INTRODUCTION .....	1
1.1.Aim .....	4
1.2.Objectives of the study .....	4
1.3. Research questions.....	4
1.4.Thesis Outline .....	4
CHAPTER TWO.....	6
DISCRIMINATING COMMERCIAL FOREST SPECIES USING IMAGE TEXTURE COMPUTED FROM A WORLDVIEW-2 PAN-SHARPENED IMAGE AND PARTIAL LEAST SQUARES DISCRIMINANT ANALYSIS .....	6
Abstract.....	7
2.1. Introduction.....	7
2.2. Material and methods .....	10
2.2.1. Study Area .....	10
2.2.2. Image Acquisition.....	10
2.2.3. Field data collection.....	11
2.2.4. Image texture analysis .....	11
2.2.5. Vegetation indices .....	13
2.2.6. Statistical analysis.....	15
2.2.6.1.Partial least squares discriminant analysis (PLS-DA) .....	15
2.2.6.2. Variable Importance in the Projection .....	15
2.2.6.3. Optimizing the PLS-DA model .....	16
2.2.7. Accuracy assessment .....	16
2.3. Result .....	17



2.3.1. Optimizing the PLS-DA model .....	17
2.3.2. Performance of image texture, vegetation indices and spectral data models .....	18
2.3.3. Frequency of selected significant variables for the PLS-DA models.....	20
2.3.4. Mapping the distribution of commercial forest species .....	21
2.4. Discussion.....	22
2.5. Conclusion .....	24
2.6. Link to next chapter .....	25
CHAPTER THREE .....	26
UTILITY OF TEXTURE COMBINATIONS COMPUTED FROM FUSED WORLDVIEW-2 IMAGERY IN DISCRIMINATING COMMERCIAL FOREST SPECIES .....	26
Abstract.....	27
3.1. Introduction.....	27
3.2. Material and methods .....	30
3.2.1. The study area.....	30
3.2.2. Image acquisition.....	31
3.2.3. Field data collection.....	32
3.2.4. Image Texture.....	33
3.2.5. Statistical analysis.....	35
3.2.5.1.Partial least squares discriminant analysis (PLS-DA) .....	35
3.2.5.2.Variable importance in the projection .....	35
3.2.5.3.Sparse partial least squares discriminant analysis (SPLS-DA) .....	36
3.2.5.4.Optimization of PLS-DA and SPLS-DA models .....	37
3.2.6. Accuracy assessment .....	37
3.3. Results .....	38
3.3.1. Optimizing the PLS-DA model .....	38
3.3.2. PLS-DA and VIP .....	39
3.3.3. SPLS-DA model optimization.....	39
3.3.4. Testing and Applying the principal component analysis (PCA) to discriminate commercial forest species for comparative purposes.....	41
3.3.5. Frequency of selected significant variables for the SPLS-DA model.....	41
3.3.6. Mapping the distribution of commercial forest species using SPLS-DA.....	42
3.4. Discussion.....	43

3.5. Conclusion .....	45
CHAPTER FOUR .....	46
4. SYNTHESIS .....	46
4.1. Introduction.....	46
4.2. Aim and objectives reviewed.....	46
4.2.1. Aim .....	46
4.2.2. Objectives reviewed .....	47
4.3. Conclusions .....	48
4.4. The future.....	49
References.....	50

## List of Figures

<b>Figure 2.1.</b> Sappi Hodgsons Estate in KwaZulu-Natal, South Africa. ....	10
<b>Figure 2.2:</b> The flowchart of the research methodology .....	17
<b>Figure 2.3.</b> Testing the discriminatory ability of each PLS-DA component using selected VIP parameters. The lowest error based on the training (n = 168) dataset was established using the cross-validation error. The arrows indicate that the components with the lowest error were the 5 <sup>th</sup> , 6 <sup>th</sup> and 7 <sup>th</sup> components for the image texture, vegetation indices and spectral band models, respectively. ....	18
<b>Figure 2.4:</b> Iterations of PLS-DA a. image texture, b. vegetation indices and c. spectral bands. ....	20
<b>Figure 2.5.</b> Frequency of parameters using PLS-DA models. ....	21
<b>Figure 2.6.</b> Species classification map produced by PLS-DA and image texture parameters .....	22
<b>Figure 3.1.</b> Location of the study area within KwaZulu-Natal Province, South Africa .....	31
<b>Figure 3.2.</b> Summary of workflow followed in this study. ....	38
<b>Figure 3.3.</b> Testing the discriminatory capability of individual PLS-DA components using texture combinations. The black arrow shows the component with the lowest error. ....	39
<b>Figure 3.4.</b> PLS-DA classification accuracies produced based on 100 iterations for splitting the training and validation data. ....	39
<b>Figure 3.5.</b> Testing the discriminatory capability of individual SPLS-DA components using texture combinations. The black arrow shows the component with the lowest error. ....	40
<b>Figure 3.6.</b> SPLS-DA classification accuracies produced based on 100 iterations for splitting the training and validation data. ....	41
<b>Figure 3.7.</b> Species classification map produced by SPLS-DA model and image texture combinations .....	43

## List of Tables

<b>Table 2.1:</b> Characteristics of the WorldView-2 pan-sharpened bands .....	11
<b>Table 2.2:</b> GLOM image texture parameters. ....	12
<b>Table 2.3:</b> GLCM image texture parameters. ....	13
<b>Table 2.4:</b> Vegetation indices tested in this study .....	14
<b>Table 2.5:</b> Accuracy results for the commercial forest classifications for each dataset. ....	19
<b>Table 3.1:</b> Characteristics of the WorldView-2 pan-sharpened bands .....	32
<b>Table 3.2:</b> Sample size of each species surveyed ( $n = 240$ ) .....	32
<b>Table 3.3:</b> Filters for the second-order texture parameters .....	34
<b>Table 3.4:</b> Classification results for discriminating commercial forest species using the SPLS-DA and PLS-DA models. ....	41
<b>Table 3.5:</b> Top 10 selected image texture combinations for the SPLS-DA model .....	42

## CHAPTER ONE

### 1. GENERAL INTRODUCTION

---

Approximately 1.2 million hectares of the South African land surface is covered by commercial forest plantations in five of the nine provinces, namely; Mpumalanga, Limpopo, KwaZulu-Natal, Western Cape and Eastern Cape (DAFF., 2012). Generally, they are dominated by pine (49%), eucalyptus (43%) and a small amount of wattle (7%) (DAFF, 2012).

These forests provide valuable environmental and economic benefits that include maintenance of the local, regional and global ecological balance, promotion of biological evolution and community succession, carbon sequestration and regulation of carbon balance and provision of ecosystem services like pollination and preservation of water catchments (DAFF., 2012). The commercial forest industry is also regarded as a key driver of the country's economy (DAFF., 2012). For instance, DAFF (2012) noted that the forestry industry alone provides over 158 000 jobs and constitutes approximately 2% (R69 billion) of the country's gross domestic product (DAFF., 2012). Therefore, understanding the composition and distribution of commercial forests is not only important for the economy, but also for making informed forest management decisions that include monitoring ecosystem health, species management practices, and harvest scheduling (Mngadi et al., 2019).

In the recent past, the commercial forestry sector has been faced with considerable pressure from population growth and resultant degradation and increased demand for agricultural and housing land. Hence, forest managers have adopted different approaches to restore, protect and maintain forest productivity while facilitating their sustainable provision of ecosystems goods and services. Such approaches involve an understanding of traditional methods such as periodic surveys, field data surveys, and aerial photographs, among others (Peerbhay et al., 2013a). However, the shortcoming of such approaches have been widely documented in literature (Nichol et al., 2010). Therefore, there is still a need for relatively accurate, timely, affordable and efficient methods of assessing commercial forests (Dube et al., 2014, Dube et al., 2015, Lottering et al., 2016). Remotely sensed earth observation data offer a great opportunity for monitoring forests. In comparison to other forest inventorying methods, such data sets are relatively inexpensive and less

tedious for assessing and observing tree species while delivering exceptional accuracy (Lottering and Mutanga, 2012, Bastin et al., 2014, Barbosa et al., 2014, Sarker and Nichol, 2011, Dube et al., 2014, Dube et al., 2015). Typically, over different spatial and temporal scales, earth observation data facilitate timely and continuous ecosystem observations. A number of studies (Mutanga and Skidmore, 2004, Ingram et al., 2005, Lu, 2006, Godsmark, 2008, Mutanga et al., 2012, Dube et al., 2014, Nichol et al., 2010, Sarker and Nichol, 2011, Peerbhay et al., 2013a, Peerbhay et al., 2013b, Mngadi et al., 2019) have successfully detected and mapped commercial forest plantations by adopting earth observation image data.

Although conventional multispectral data have been particularly useful in forest species mapping and discrimination, it has been noticed that the utilization of their broadband multispectral sensors produced generalized classifications that are not helpful to forest researchers and managers (Yu et al., 2006). Therefore, the emergence of the new generation multispectral sensors (e.g., WorldView2, RapidEye and GeoEye), with greater spatial resolutions and strategically placed bands, are likely to enhance tree species delineation (Peerbhay et al., 2013b). As a result, this study aims to explore the effectiveness of WorldView-2 pan-sharpened multispectral imagery for mapping commercial forest species. Pan-sharpening is an image enhancement process where a panchromatic high spatial resolution image is merged with a medium spatial resolution multispectral image to generate a higher spatial resolution image. This technique was utilized in this study to improve the spatial resolution of the image, while maintaining its spectral information (Kpalma et al., 2014). Although literature has indicated that remotely sensed data has successfully delineated forest species in the past, these studies have centred their attention on the use of spectral data and vegetation indices to detect and map commercial forest species. Generally, these approaches have produced reasonable classification accuracies, but with a number of limitations (Anderson et al., 1993, Dube et al., 2014, Dube et al., 2015, Hlatshwayo et al., 2019). For example, canopy shadow and changing vegetation growth affects spectral vegetation indices immensely, especially NDVI, which saturates at dense biomass levels (Nichol et al., 2010, Dube et al., 2015, Hlatshwayo et al., 2019). These challenges have led to the exploration of approaches that are not affected by vegetation growth or saturation. Therefore, the use of image texture has become increasingly appealing as a solution for the challenges encountered by vegetation indices and spectral data (Fuchs et al., 2009, Nichol et al., 2010, Sarker and Nichol, 2011, Dube et al., 2015).

In commercial forestry, texture has been utilized to identify different forest stand structure characteristics, which include; age, density, and leaf area index from medium-to-high spatial resolution images (Moskal and Franklin, 2004, Sarker and Nichol, 2011). The major strength of adopting image-texture is the increased capacity to streamline and simplify complex canopy structures (Nichol et al., 2010, Sarker and Nichol, 2011, Dube et al., 2015, Lottering et al., 2020). Although, image texture has shown a reasonable degree of accuracy, research have shown that the method is unable to manage issues related to sensor angle, topographic effects and radiance from the sun (Dube et al., 2015, Hlatshwayo et al., 2019, Lottering et al., 2019). Therefore, studies have recently introduced texture combinations to map forest species. The use of texture band combinations has achieved a high degree of success in forest species mapping, especially when compared to raw texture bands and vegetation indices (Hlatshwayo et al., 2019, Lottering et al., 2019). The utilization of texture combinations has been outstanding in detecting and mapping forest plantations, in contrast to vegetation indices and raw texture bands (Dube et al., 2015).

However, when dealing with intricate data such as texture combinations whereby data dimensionality is extremely high and very difficult to manage, it is worth saying that a robust feature extraction technique is needed to deal with these issues. Therefore, partial least squares discriminant analysis (PLS-DA) would be a suitable algorithm to overcome the difficulties of textural data, due to its excellent display to curb background effects and its ability to manage spectral similarities between tree species. Also, PLS has the capability to store data into few PLS latent components (Peerbhay et al., 2014, Chetty, 2020), keeping important texture parameters for later use. However, this process does not occur simultaneously and is dependent on the variable importance in the projection (VIP) for this to occur. Furthermore, it is worth noting, the issue of simultaneous variable selection remains when using PLS-DA. Therefore, there is a need for a novel approach that can perform simultaneously variable selection without relying on VIP such as the sparse partial least squares discriminant analysis (SPLS-DA), which needs to be tested for effectively detecting commercial forest species using image texture. SPLS-DA presents an opportunity to reliably map forest plantations and it has proven to be able to deal with complex textural datasets (Lottering et al., 2020).

### **1.1.Aim**

The aim of this study was to discriminate commercial forests species using image texture computed from a 0.5m WorldView-2 pan-sharpened image.

### **1.2.Objectives of the study**

The study objectives were as follows:

- To discriminate commercial forest species using image texture computed from a 0.5 m WorldView-2 pan-sharpened image and partial least squares discriminate analysis.
- To explore the utility of texture combinations computed from fused WorldView-2 imagery in discriminating commercial forest species.

### **1.3. Research questions**

- Can image texture and PLS-DA detect and map commercial forest species?
- Does image texture combinations in conjunction with SPLS-DA effectively discriminate forest species?

### **1.4.Thesis Outline**

This thesis consists of two articles that have been submitted for peer review to Remote Sensing Applications: Society and Environment and Geocarto International. Both journal papers have been published online. These articles are presented as individual chapters in the thesis and each chapter comprises an introduction, methods, results, discussion, and conclusion. This thesis constitutes four chapters. Chapter one is the general introduction, chapter two and three are Journal articles and finally chapter four is the synthesis.

**Chapter One:** This is an introductory chapter which explains the importance of the study. Specifically, the aim, objectives, scope, and outline of the thesis are provided. Furthermore, this chapter contextualizes the research questions.

**Chapter Two:** This chapter explores the potential of image texture using various moving window sizes to discriminate commercial forest species. Furthermore, the chapter compares the image texture model with vegetation indices and raw spectral bands to determine which model better classifies commercial forest species.



**Chapter Three:** This chapter is an extension of chapter two and explores the value of texture combinations in discriminating commercial forest species. The chapter explores the utility of texture combinations computed from WorldView-2 imagery in conjunction with PLS-DA and SPLS-DA for discriminating commercial forest species.

**Chapter Four:** The last chapter is the conclusion, which evaluates and highlights the main findings of the two previous chapters.

## CHAPTER TWO

### DISCRIMINATING COMMERCIAL FOREST SPECIES USING IMAGE TEXTURE COMPUTED FROM A WORLDVIEW-2 PAN-SHARPENED IMAGE AND PARTIAL LEAST SQUARES DISCRIMINANT ANALYSIS

---

This chapter is based on:



Bongokuhle Sibiyi, Romano Lottering & John Odindi, 2021. Discriminating commercial forest species using image texture computed from a WorldView-2 pan-sharpened image and partial least squares discriminant analysis. *Remote Sensing Applications: Society and Environment*, p.100605.

## Abstract

Discriminating forest species is crucial for effective management of commercial forest plantations. Whereas several variants of vegetation indices have commonly been used to delineate forest species, their efficacy is impeded by saturation at high biomass levels. However, image texture does not suffer from saturation at high biomass levels, hence offers a unique opportunity to reliably map commercial forest species typically characterized by dense canopies. In this study, we integrated image texture computed from a 0.5 m WorldView-2 pansharpened image with partial least squares discriminant analysis (PLS-DA) to detect and map commercial forest species. The results illustrated that the image texture (overall accuracy (OA) = 77%, kappa = 0.69) outcompeted both the vegetation indices (OA = 69%, kappa = 0.59) and raw spectral bands models (OA = 64%, kappa = 0.52). PLS-DA together with variable importance in the projection selected homogeneity, correlation and mean as the most significant texture parameters, which were predominantly computed from the red-edge, near infrared (NIR) 1 and 2 bands. Furthermore, PLS-DA model commonly selected the  $7 \times 7$  than the  $3 \times 3$  and  $5 \times 5$  moving windows. Overall, this study demonstrates the ability of image texture in discriminating commercial forest species.

**Keywords:** Image texture, species discrimination, PLS-DA, commercial forest

## 2.1. Introduction

Commercial forests cover roughly 1.5 million hectares of South Africa's landmass (DAFF, 2008, DAFF., 2012), and primarily located along the country's eastern provinces of KwaZulu-Natal and Mpumalanga (DAFF, 2008, Clarke, 2018, Lottering et al., 2020). These forests are crucial to South Africa's economy as they contribute approximately 2% of its gross domestic product, mainly through the supply of hard- and soft wood (DAFF, 2008, Peerbhay et al., 2013a, Mngadi et al., 2019). The hardwood forest consists of mainly Eucalyptus (82%) and Acacia (17%), while the softwood consists of Pine (28,7%) (DAFF., 2012). Statistics on the distribution of commercial forest species is important, to among others, the sector's economic accounting, national and international carbon emission and assimilation agreements, greenhouse effects and expediting informed forest management decisions (Sesnie et al., 2010, Peerbhay et al., 2013a, Peerbhay et al., 2013b, Dube et al., 2015, Mngadi et al., 2019). Such decisions include forest ecosystem health, harvest scheduling, site management practices and commercial output and viability. According to

Peerbhay et al. (2013a), forest species discrimination is essential for forest inventory management, forest fragmentation, conservation planning, assessment of species diversity, fire hazard monitoring and control. Hence, it is necessary to find precise and opportune methods to discriminate commercial forest species (Van Aardt and Wynne, 2007).

The use and limitations of traditional approaches used for identifying forest species such as field surveys are well documented in literature (Nichol et al., 2010, Sarker and Nichol, 2011, Dube et al., 2014, Dube et al., 2015, Mushore et al., 2017, Hlatshwayo et al., 2019, Lottering et al., 2019). Recently, remote sensing, in complementarity with field data, has emerged as a viable indirect and non-destructive option for forest inventory management (Franklin et al., 2000, Franklin, 2001, Moskal and Franklin, 2004, Ismail et al., 2008, Dye et al., 2012, Mutanga et al., 2012, Lottering et al., 2016, Dube et al., 2018, Mngadi et al., 2019). For instance, Peerbhay et al. (2013b), used WorldView-2 data to successfully discriminate commercial forest species in KwaZulu-Natal, South Africa, while Lottering et al. (2016), also successfully used WorldView-2 imagery to discriminate commercial forest vegetation, reporting an overall accuracy of 90%. Generally, these studies have adopted spectral data and vegetation indices to detect and map commercial forest species. However, the use of spectral bands is commonly limited by rapid vegetation growth and canopy shadowing while vegetation indices, such as NDVI, saturate at dense biomass levels (Lu et al., 2002, Lu and Batistella, 2005, Mather and Koch, 2011, Sarker and Nichol, 2011, Hlatshwayo et al., 2019, Lottering et al., 2019, Lottering et al., 2020). These limitations necessitate an exploration of approaches that are not compromised by vegetation growth, hence changes in foliar spectral characteristics and dense biomass saturation.

In this regard, several studies have explored the use of image texture as a solution to the shortcomings encountered by spectral and vegetation indices (Franklin et al., 1996, Franklin et al., 2000, Moskal and Franklin, 2004, Nichol et al., 2010, Sarker and Nichol, 2011, Dube et al., 2015). This interest is motivated by its ability to identify spectrally unique objects or regions of interest, which are based on the function of local variance in the image, hence scale-dependent (Hlatshwayo et al., 2019, Lottering et al., 2019, Lottering et al., 2020). Furthermore, image texture has proven effective in identifying forest stand structure characteristics that include age, density, and leaf area index (Lu and Batistella, 2005, Lottering et al., 2019, Lottering et al., 2020). According to

Champion et al. (2008), texture simplifies complex forest canopy structures, especially closed canopies, and can be used to detect fine vegetation biophysical properties.

To date, promising results have been achieved using texture analysis to detect and map spatial phenomenon. For example, Lottering et al. (2020), successfully used image texture to detect and map Bugweed (*Solanum mauritianum*) within a commercial forest plantation. Similarly, Franklin et al. (2000), incorporated texture into the classification of forest species in Alberta and New Brunswick, Canada, recording a 5% and 12% increase in the classification accuracy, respectively. However, despite these successes, potential problems in implementing image texture in discriminating forest species include texture complexity and potential variability in physiographic conditions and varying results based on selected window sizes (Marceau et al., 1990, Franklin et al., 2000, Chen\* et al., 2004, Dube et al., 2015). Furthermore, processing texture can generate a large volume of data, which can be difficult to manage (Chen\* et al., 2004). Although texture has generally shown great potential in discriminating commercial forest species, the above-mentioned challenges remain largely unexplored (Fuchs et al., 2009, Li et al., 2015). For successful image texture classification, an effective method for feature extraction is required, as image textural parameters may be characterized by high data dimensionality and redundancy (Lottering et al., 2020).

Studies have demonstrated that partial least square discriminant analysis (PLS-DA) can effectively deal with complex data, as it can reduce background effects and resolve spectral or spatial similarities between tree species (Peerbhay et al., 2013a). PLS-DA decomposes complex data into PLS latent components (Peerbhay et al., 2013b, Lottering et al., 2020), preserving the most significant texture parameters used for further investigation. This is achieved by selecting the significant predictor variables using variable importance in the projection (VIP) (Peerbhay et al., 2013a). These variables are then used as input data to increase the classification accuracy, reduce redundancy, and require less storage space when compared to other algorithms.

Therefore, in this study, we integrated image texture computed from a 0.5 m WorldView-2 pansharpened image with PLS-DA to discriminate commercial forest species. The WorldView-2 pansharpened image was selected because of its high spatial resolution, thus providing enhanced image texture information for discriminating commercial forest species. Specifically, we explored the potential of image texture using various moving windows to discriminate commercial forest

species and compared the image texture model with vegetation indices and raw spectral bands to determine which model better classified commercial forest species.

## 2.2. Material and methods

### 2.2.1. Study Area

This study was conducted in the Sappi Hodgson Estate in KwaZulu-Natal, South Africa ( $30^{\circ}59'85''$  E;  $29^{\circ}19'03''$  S) (Figure 2.1). The area covers 6391 ha and is located in the mist belt grassland bioregion of the KwaZulu-Natal midlands. The area receives summer rainfall ranging from 730 to 1590 mm per annum and is characterized by mist conditions in winter. The landscape is classified as rolling and hilly, with elevation ranging from 1030 to 1590 m above sea level. Major tree species in the estate are *A. mearnsii*, *E. dunnii*, *E. grandis* and *P. patula*.

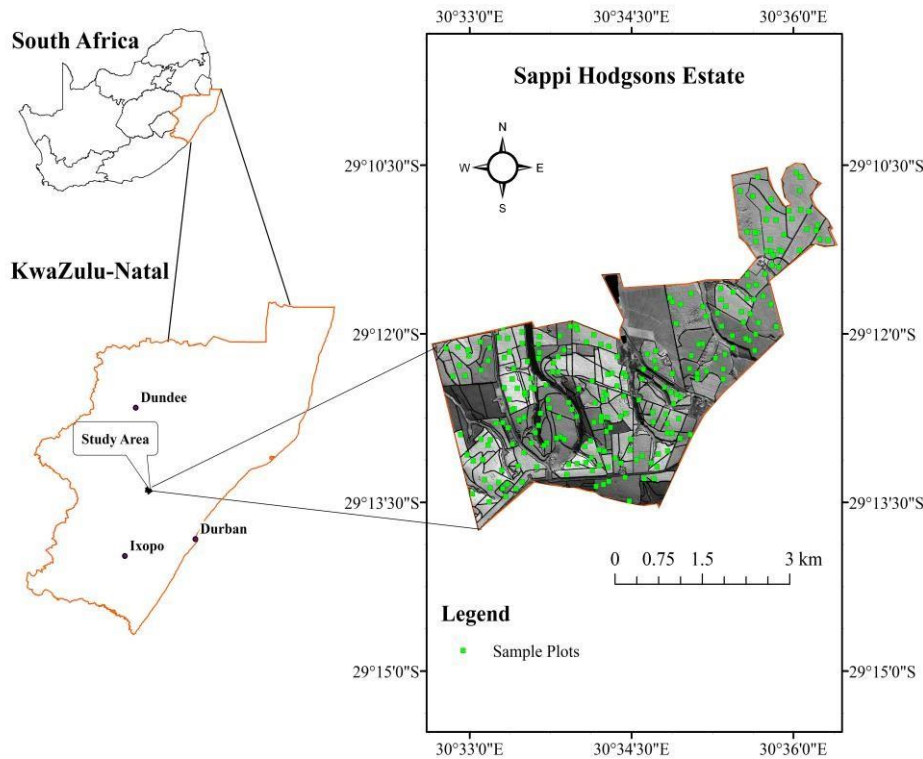


**Figure 2.1.** Sappi Hodgson Estate in KwaZulu-Natal, South Africa.

### 2.2.2. Image Acquisition

A WorldView-2 pan-sharpened image was obtained under cloudless conditions on the September 20, 2012. The WorldView-2 multispectral system comprises of eight wavebands (Table 2.1). The image was atmospherically corrected to the top-of-atmosphere reflectance using the Fast Line-of-Sight Atmospheric Spectral Hypercubes in ENVI 4.7 software. The image was then geo-rectified

to a root mean square error (RMSE) of less than one-pixel size (0.5 m) and orthorectified using twenty-five well-distributed ground control points. It was then projected to the Universal Transverse Mercator projection, using the World Geodetic System 84 datum.

**Table 2.1:** Characteristics of the WorldView-2 pan-sharpened bands

Band	Range (nm)
Coastal blue	400-450
Blue	450-510
Green	510-580
Yellow	585-625
Red	630-690
Red edge	705-745
Near-IR1	770-895
Near-IR2	860-1040

### 2.2.3. Field data collection

Six stands per species (i.e., *E. grandis*, *A. mearnsii*, *P. patula*, and *E. dunni*) were randomly selected within the study area and field visits conducted to verify the status of the selected stands. The Hawth's tool in ArcMap 10.5 was used to randomly generate  $30 \times 30$  m plots over the study area using an existing WorldView-2 image. To ensure that the sample sizes for the species were balanced and statistically representative, each stand was sub-sampled to ensure that the sample points are equally distributed. The final dataset consisted of 240 sample plots with 70% ( $n = 168$ ) used for training and the remaining 30% ( $n = 72$ ) as the test dataset. According to Peerbhay et al. (2013b), balancing the number of sample classes among training and test data is essential for optimal PLS-DA optimization. The R Studio statistical software package version 3.1.3 was used to run the data to ensure that the number of samples in the training and test datasets for the various species were approximately equal.

### 2.2.4. Image texture analysis

Texture refers to the function of local variance within an image and is dependent on the properties of neighborhood pixels (Lottering et al., 2019). The use of texture could be useful for discriminating commercial forest species as changes in the canopy structure between species could result in a variation in image texture (Lottering et al., 2020). Although several studies have noted the potential of image texture as a source of information for high spatial resolution imagery (Moskal and Franklin, 2004, Lottering et al., 2020), there is a dearth in literature demonstrating its

use. Furthermore, several texture analyses tools have been recently developed to extract features from an image (Li et al., 2015). In this study, the Grey Level Occurrence Matrix (GLOM) (Table 2.2) and Grey Level Co-occurrence Matrix (GLCM) (Table 2.3) were utilized to extract texture from the WorldView-2 pan-sharpened image. With the use of GLOM, texture is calculated using the pixel intensities of the histogram within a processing window. The GLOM does not consider the spatial relationship between pixels (St-Louis et al., 2006, Hlatshwayo et al., 2019, Lottering et al., 2019).

**Table 2.2:** GLOM image texture parameters.

Parameter	Formula	Description
Data Range	$\max\{X\} - \min\{X\}$ Where $X = x_1, x_2, \dots, x_k$	Computes the data range of the pixel (St-Louis et al., 2006).
Entropy	$\sum_{i=0}^{N-1} p(i) \log_2 [p(i)]$ Where $N$ is the total number of intensity levels	Determines histogram (Materka and Strzelecki, 1998).
Mean	$AVG = \frac{\sum_k X_k}{K}$	Estimates the mean texture value (Lottering et al., 2019).
Skewness	$\mu_3 = \sigma^{-3} \sum_{i=0}^{N-1} (i - \mu)^3 p(i)$ Where $N$ is the total number intensity levels.	Establishes the skewness of the data (Materka and Strzelecki, 1998).
Variance	$\frac{\sum (x_{ij} - M)^2}{n - 1}$ Where $x_{ij}$ is the digital number of the pixel $(i, j)$ , and $n$ is the number of pixels in the moving window.	Focuses on the variability of the spectral response of pixel (Lottering et al., 2019).

On the other hand, GLCM uses all pairwise combinations of grey levels within a window (Hlatshwayo et al., 2019). According to Lottering et al. (2019), a set of grey-level co-occurrence probabilities are stored and statistics applied to the matrix to generate image texture parameters. Table 2.3 provides a brief description of GLCM image texture parameters.



**Table 2.3:** GLCM image texture parameters.

Parameter	Formula	Description
Contrast	$\sum_{i,j=0}^{N-1} P_{i,j}(i-j)^2$	Determines the level of local variation within a window (Yuan et al., 1991).
Correlation	$\frac{\sum_{i,j=0}^{N-1} P_{i,j} \frac{(i-\mu_i)(j-\mu_j)}{\sqrt{(\sigma_i^2)(\sigma_j^2)}}}{\sqrt{(\sigma_i^2)(\sigma_j^2)}}$	Estimates the grey-level linear dependency in an image (Lottering et al., 2019).
Dissimilarity	$\sum_{i,j=0}^{N-1} P_{i,j} i-j $	Establishes local variation (Rubner et al., 2001).
Entropy	$\sum_{i,j=0}^{N-1} P_{i,j}(-\ln P_{i,j})$	Measures statistical uncertainty (Yuan et al., 1991)
Homogeneity	$\sum_{i,j=0}^{N-1} \frac{P_{i,j}}{1+(i-j)^2}$	Determines smoothness of texture (Haralick et al., 1973)
Mean	$\mu_i = \sum_{i,j=0}^{N-1} i(P_{i,j})$ $\mu_j = \sum_{i,j=0}^{N-1} j(P_{i,j})$	Mean grey-level within a small neighborhood (Materka and Strzelecki, 1998).
Second moment	$\sum_{i,j=0}^{N-1} P_{i,j}^2$	Indicators local homogeneity (Yuan et al., 1991).
Variance	$\sigma_i^2 = \sum_{i,j=0}^{N-1} P_{i,j}(i-\mu_i)^2$ $\sigma_j^2 = \sum_{i,j=0}^{N-1} P_{i,j}(j-\mu_j)^2$	Variability of the spectral response of pixels (Haralick et al., 1973)

In this study, these texture parameters were computed from a 0.5 m WorldView-2 pan-sharpened image to determine their potential in discriminating commercial forest species with a cooccurrence shift of  $x = 1$ ,  $y = 1$  and  $\theta = 45^\circ$ . A  $45^\circ$  angle was found to be suitable in calculating image texture parameters to classify commercial forestry. It is worth noting that texture features are identified with a moving window to show the connection between a pixel and its neighbour (Li et al., 2015). In this study, three moving windows (i.e.,  $3 \times 3$ ,  $5 \times 5$  and  $7 \times 7$ ) were adopted. The image texture parameters were computed using ENVI 4.7 software and mean value for each texture parameter extracted in ArcGIS 10.5, which corresponded with the 240 sample plots.

### 2.2.5. Vegetation indices

Eighteen vegetation indices reported in literature were selected and tested to discriminate commercial forest species (Table 2.4). These indices were generally dependent on the red, rededge and NIR regions of the electromagnetic spectrum. The selected indices have shown to be effective

in classifying commercial forest species, and most are particularly sensitive to the reflectance in the visible and NIR regions (Lottering et al., 2018). The choice of these indices was based on previous studies that demonstrated their reliability in classifying vegetation (Adelabu et al., 2013, Mushore et al., 2017). Also, the emphasis was placed on vegetation indices with wavelengths within the red-edge region, as it is known to be useful in determining vegetation health and vegetation classification (Barry et al., 2008, Eitel et al., 2011).

**Table 2.4:** Vegetation indices tested in this study

<b>Vegetation index</b>	<b>Abbreviation</b>	<b>Equation</b>	<b>Reference</b>
Normalized Difference Vegetation Index	NDVI	$\frac{(NIR-RED)}{(NIR+RED)}$	(Lottering et al., 2018)
Simple ratio	SR	$\frac{NIR}{RED}$	(Lottering et al., 2018)
Enhanced vegetation index	EVI	$\frac{2.5 * (NIR-RED)}{(NIR+6*RED-7.5*BLUE+1)}$	(Huete et al., 2002).
Red green ratio	RGR	$\frac{RED}{GREEN}$	(Gamon and Surfus, 1999)
Difference vegetation index	DVI	$NIR - RED$	(Lottering et al., 2018)
Atmospherically resistance vegetation index	ARVI	$\frac{(NIR-RED)}{(NIR+BLUE)}$	(Kaufman and Tanre, 1996)
Plant senescence reflectance index	PSRI	$\frac{RED - BLUE}{RED\ EDGE}$	(Sims and Gamon, 2002)
Green normalized difference vegetation index	GNDVI	$\frac{(NIR-GREEN)}{(NIR+GREEN)}$	(Ahamed et al., 2011)
Green difference vegetation index	GDVI	$NIR - GREEN$	(Sripada et al., 2006)
Transformed difference vegetation index	TDVI	$\sqrt{0.5 + \frac{(NIR - RED)}{(NIR + RED)}}$	(Bannari et al., 2002)
Soil adjusted vegetation index	SAVI	$\frac{1.5*(NIR-RED)}{(NIR+RED+0.5)}$	(Lottering et al., 2018)
Datt/Maccioni index	DMI	$\frac{(NIR-RED\ EDGE)}{(NIR-RED)}$	(Maccioni et al., 2001)
Red Edge yellow ratio	REY	$\frac{RED\ EDGE-YELLOW}{REDEGE+YELLOW}$	(Gwata, 2012)
Red Edge NDVI	NDRE	$\frac{NIR-REDEGE}{NIR+REDEGE}$	(Lottering et al., 2018)
Modified triangular vegetation index	MTVI2	$\frac{1.5(1.2(NIR-GREEN)-2.5(RED - GREEN))}{\sqrt{((2NIR + 1)^2 - (6NIR - 5\sqrt{RED}) - 0.5)}}$	(Haboudane et al., 2004)
Red Edge simple ratio	Srre	$\frac{NIR}{RED\ EDGE}$	(Lottering et al., 2018)
Green ratio vegetation index	GRVI	$\frac{NIR}{GREEN}$	(Lottering et al., 2018)
Modified chlorophyll absorption ratio index 2	MCARI2	$\frac{1.5[2.5(NIR-RED)-1.3(NIR-GREEN)]}{\sqrt{((2NIR + 1)^2 - (6NIR - 5\sqrt{RED}) - 0.5)}}$	(Haboudane et al., 2004)

## 2.2.6. Statistical analysis

### 2.2.6.1. Partial least squares discriminant analysis (PLS-DA)

The partial least squares discriminant analysis (PLS-DA) is dependent on the classical partial least squares regression method as a basis for constructing predictive models (Peerbhay et al., 2013b, Sibanda et al., 2015). PLS regression provides dimension reduction in an application where the response variable (Y) is related to the predictor variables (X). In the case of PLS-DA, the response variable (i.e. forest species) is binary and expresses class membership (Sibanda et al., 2015). The PLS-DA algorithm is expressed by the equations (Peerbhay et al., 2013b):

$$\mathbf{X} = \mathbf{TP}' + \mathbf{E} \quad (1)$$

$$\mathbf{Y} = \mathbf{UQ}' + \mathbf{F} \quad (2)$$

Where;  $\mathbf{X}$  = the matrix of the wavebands,  $\mathbf{T}$  = factor score matrix,  $\mathbf{P}$  =  $\mathbf{X}$  loadings and  $\mathbf{E}$  = residual or a noise term.  $\mathbf{Y}$  = matrix of the response variable (forest species),  $\mathbf{U}$  = scores for  $\mathbf{Y}$ ,  $\mathbf{Q}$  =  $\mathbf{Y}$  loadings, and  $\mathbf{F}$  = residual for  $\mathbf{Y}$  (Peerbhay et al., 2013a, Lottering et al., 2020). In the R statistical package version 3.1.3 (Team, 2013), the “plsda” function was used to run the PLS-DA algorithm.

### 2.2.6.2. Variable Importance in the Projection

PLS-DA is dependent on variable importance in the projection (VIP) to select the most important wavebands or texture parameters, producing a score for measuring the most important parameters. The VIP is defined as follows (Peerbhay et al., 2013b):

$$VIP_k = \sqrt{K \sum_{a=1}^A [(q_a^2 t_a^T t_a)(w_{ak}/\|w_k\|^2)] / \sum_{a=1}^A (q_a^2 t_a^T T_a)} \quad (3)$$

where  $VIP_k$  represents the importance of the  $k$ 'th texture parameters constructed by the PLS-DA model with a component,  $w_{ak}$  represents the consistent loading weight of the  $k$ th texture parameters in the  $a$ 'th PLS-DA component,  $t_a$ ,  $w_a$ , and  $q_a$  are the  $a$ 'th column vectors and  $K$  the total number of texture parameters. PLS-DA model is identified by those texture measures that have a VIP score of greater than 1. Selected VIP texture parameters were then used to create a new PLS-DA model, which was used for classifying the test dataset. Using the R statistical package version 3.1.3 (Team, 2013), the “vip” function was used to run VIP for selecting significant variables.

#### *2.2.6.3. Optimizing the PLS-DA model*

To select the optimal number of components using the training dataset, it is important to obtain a PLS-DA model with accurate classification performance. A tenfold cross-validation (CV) method was utilized to determine the number of components required for the PLS-DA model. The number of components were sequentially increased until the CV error became stable, achieved when further components did not change the classification output. Once the point of stability was reached, the selected number of components were used to classify the test dataset (Lottering et al., 2020).

#### *2.2.7. Accuracy assessment*

The results of the classification were calculated using the confusion matrix that was based on the test dataset. The calculation of the confusion matrix was accomplished by dividing the entire dataset (240) into training data (70%) and test data (30%) using a repeated holdout sample with 100 repetitions. Class accuracies for individual forest species were also compared by examining the user's and producer's accuracies. Furthermore, the kappa analysis was utilized as it compares observed accuracy and predictable accuracy. This measure uses the  $k$  (KHAT) statistic, where coefficients closer to or equal to one assume perfect agreement (Peerbhay et al., 2013a, Peerbhay et al., 2013b, Mngadi et al., 2019). Figure 2.2 shows a flowchart of the methodology undertaken in this study.

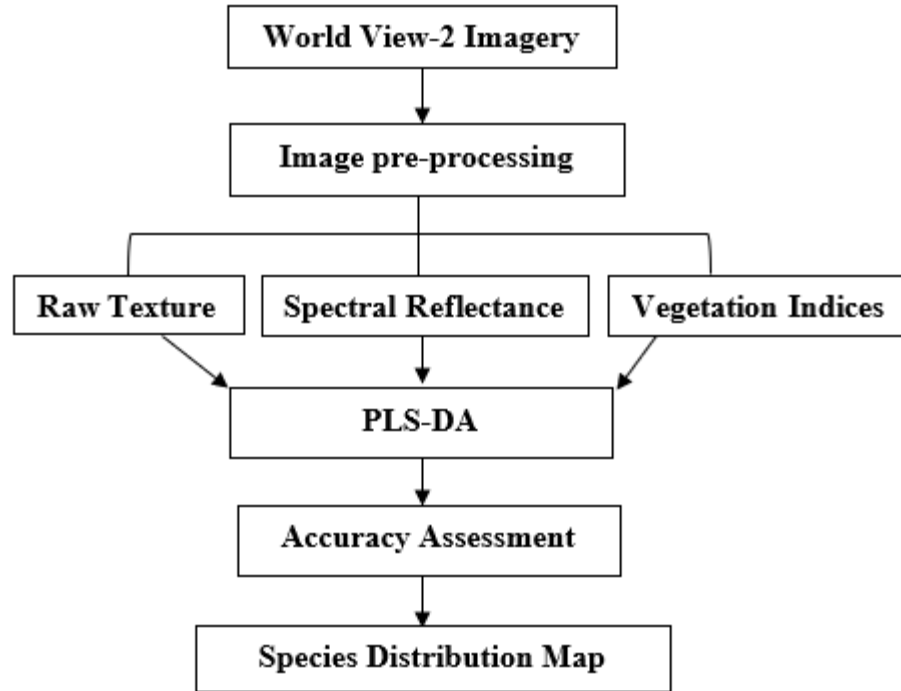


**Figure 2.2.** The flowchart of the research methodology

## 2.3. Result

### 2.3.1. *Optimizing the PLS-DA model*

Figure 2.3 shows the number of components used to develop the PLS-DA model for discriminating commercial forest species. In this study, the lowest percentage was achieved using a tenfold crossvalidation error method to determine the number of components in the model with the lowest error rate based on the training ( $n = 168$ ) dataset. The results showed that the 5<sup>th</sup>, 6<sup>th</sup>, and 7<sup>th</sup> component had the lowest error for the image texture, vegetation indices and spectral band models, respectively. Therefore, these components were used to develop the PLS-DA model and the calculation of VIP scores for each parameter.

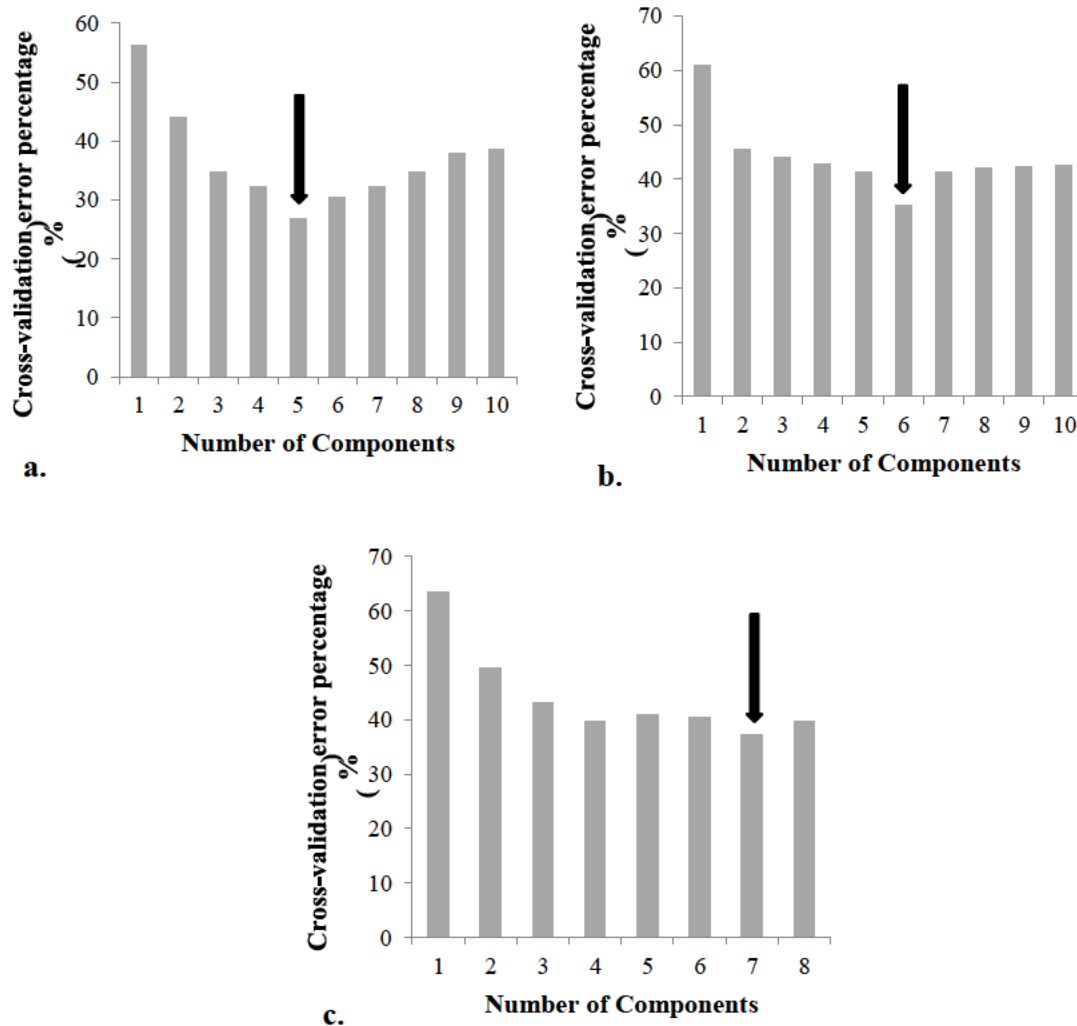


**Figure 2.3.** Testing the discriminatory ability of each PLS-DA component using selected VIP parameters. The lowest error based on the training ( $n = 168$ ) dataset was established using the cross-validation error. The arrows indicate that the components with the lowest error were the 5<sup>th</sup>, 6<sup>th</sup> and 7<sup>th</sup> components for the image texture, vegetation indices and spectral band models, respectively.

### 2.3.2. Performance of image texture, vegetation indices and spectral data models

Table 2.5 shows that the PLS-DA model using image texture yielded the highest classification accuracy, followed by the PLS-DA model using vegetation indices and lastly the PLS-DA model using the WorldView-2 spectral bands.

**Table 2.5:** Accuracy results for the commercial forest classifications for each dataset.

Accuracy measurements		Models		
		Spectral data	Vegetation indices	Image texture
<i>A. mearnsii</i>	User's accuracy	72	73	72
	Producer's accuracy	81	81	90
<i>E. dunnii</i>	User's accuracy	58	70	68
	Producer's accuracy	57	74	80
<i>E. grandis</i>	User's accuracy	40	62	80
	Producer's accuracy	53	54	70
<i>P. patula</i>	User's accuracy	87	72	88
	Producer's accuracy	63	70	74
Overall accuracy		<b>64%</b>	<b>69%</b>	<b>77%</b>
Kappa coefficient		<b>0.52</b>	<b>0.59</b>	<b>0.69</b>

Figure 2.4 illustrates the change in overall accuracy produced by each model when run at 100 iterations for dividing the test and train datasets. The mean overall classification accuracy and standard deviation was 69% and 2.2, respectively for image texture model, 77% and 2.2, respectively for vegetation indices model and 64% and 2.0, respectively for the spectral bands model.

In addition, we also ran a McNemar's test between the models to establish whether the PLS-DA image texture model statistically improved the overall classification accuracy over the PLS-DA vegetation indices model and the PLS-DA spectral bands model. The following hypotheses were tested: the null hypothesis  $H_0$ : there were no significant differences in accuracy between the models ( $p > 0.05$ ) versus the alternate hypothesis  $H_a$ : there was a significant difference in accuracy between the models ( $p < 0.05$ ). We subsequently rejected the null hypothesis as there was a significant difference between the models ( $p < 0.05$ ).

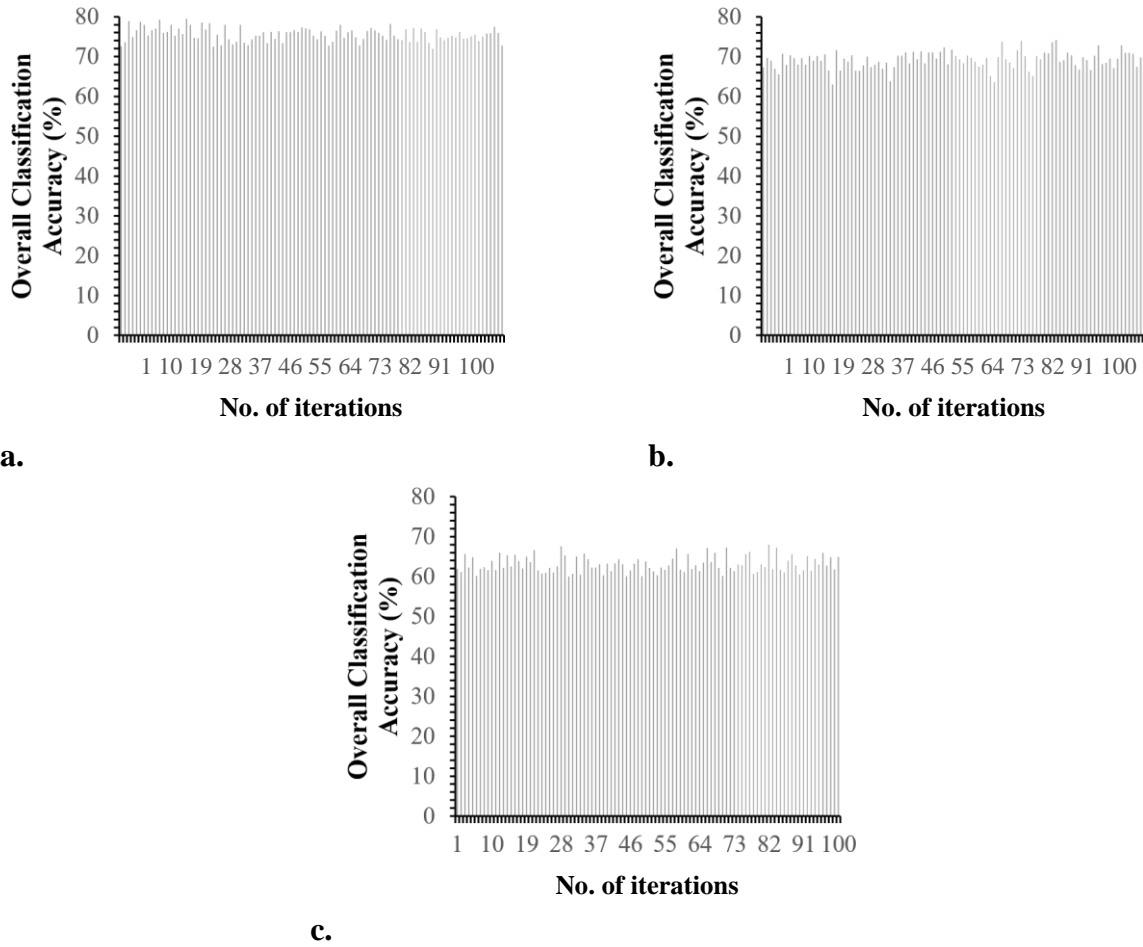


**Figure 2.4.** Iterations of PLS-DA a. image texture, b. vegetation indices and c. spectral bands.

### 2.3.3. Frequency of selected significant variables for the PLS-DA models

Since the PLS-DA image texture model was the most significant performer, we only illustrated the frequency of this model's parameters. Figure 2.5 shows the frequency of significant parameters selected by VIP for developing the PLS-DA image texture model. Figure 2.5a shows that the rededge, NIR1 and NIR2 bands were the most significant in developing texture parameters. Figure 2.5b shows that the  $7 \times 7$  moving window was the most significant in model development while Figure 2.5c shows that homogeneity, correlation and mean texture parameters contained most of the commercial species information. In addition, Figure 2.5d shows that the VIP frequently selected co-occurrence image texture parameters than the occurrence image texture parameters.



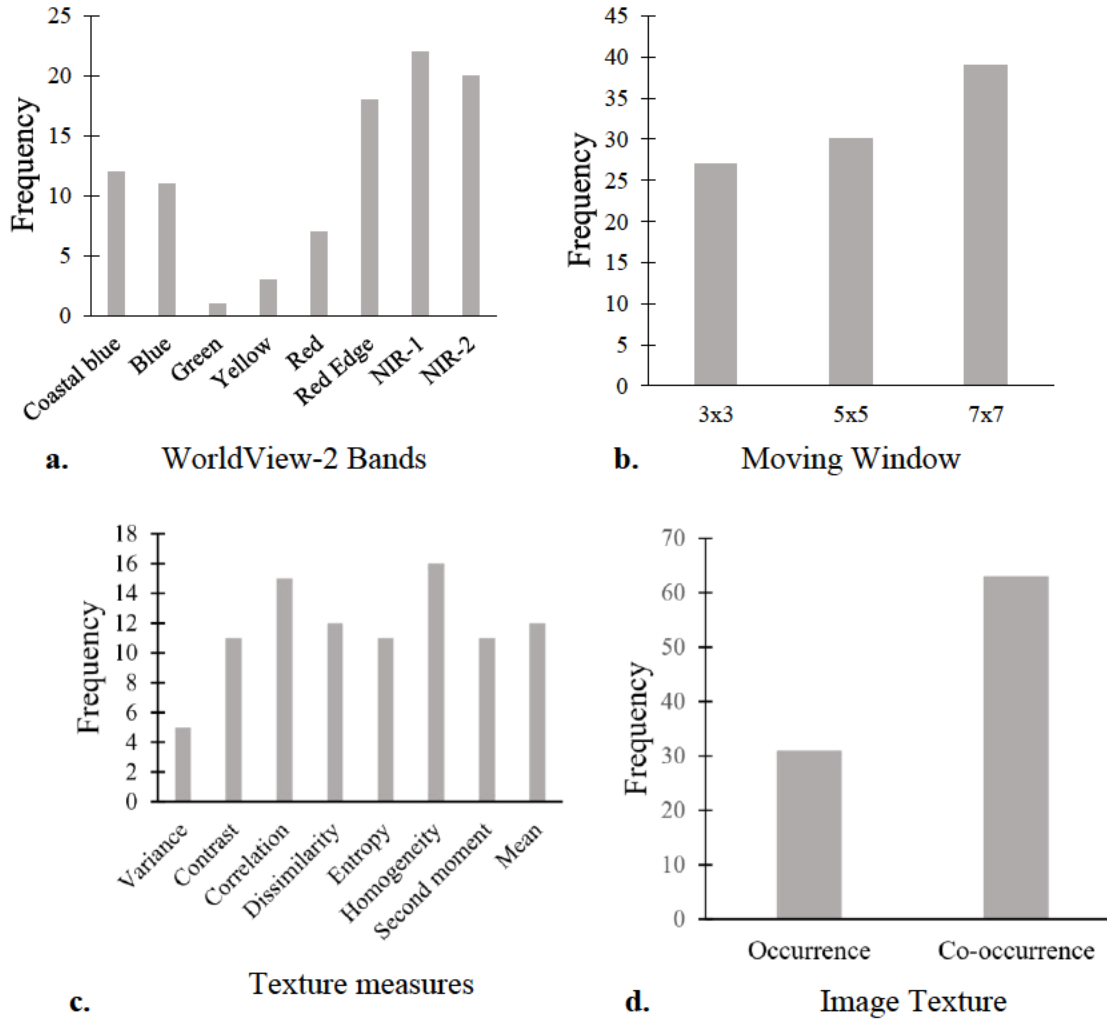


**Figure 2.5.** Frequency of parameters using PLS-DA models.

#### 2.3.4. Mapping the distribution of commercial forest species

Since the PLS-DA image texture model produced the highest overall accuracy, we used this model to map the spatial distribution of commercial forest species. Figure 2.6 shows the distribution of various commercial species over the study area, with *P. patula* and *A. mearnsii* the most correctly classified species. In contrast, *E. dunni* and *E. grandis*, have the most confusion (texture similarities) with each other, this is due to both species belonging to the same genus, hence, least correctly mapped species, respectively.

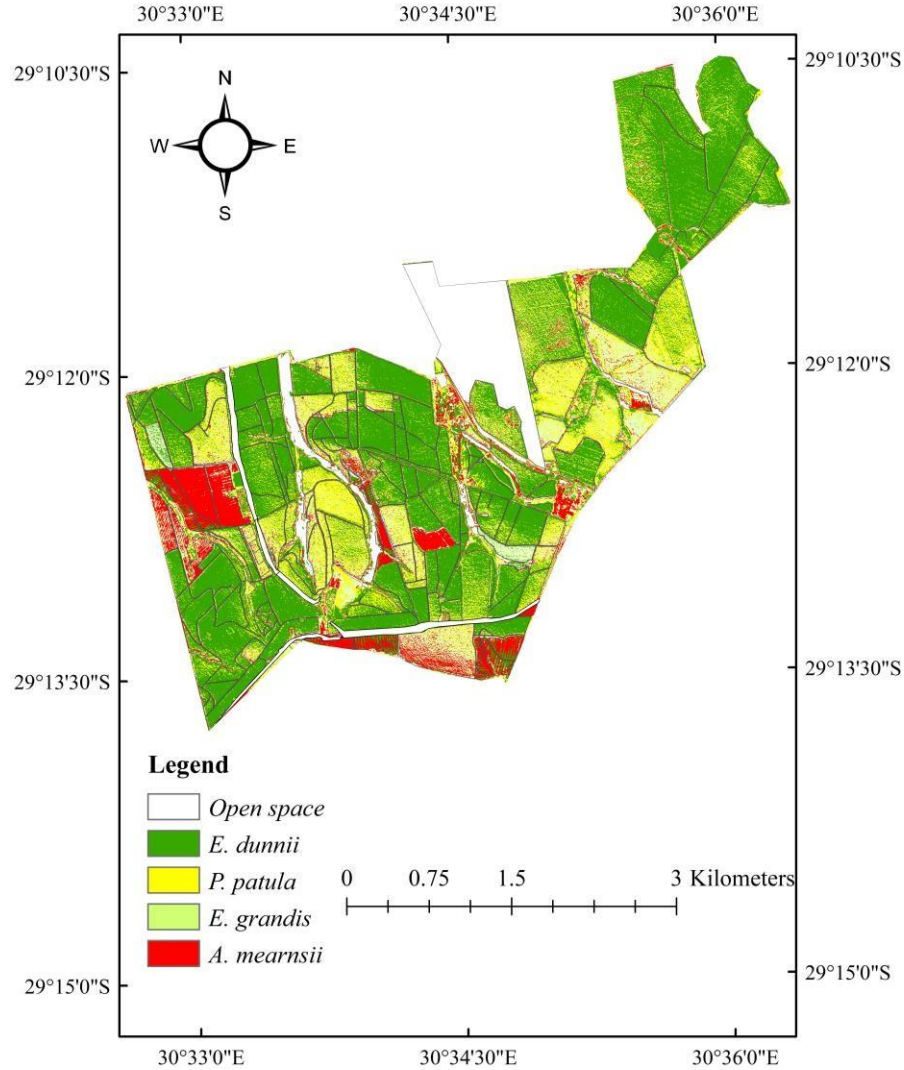


**Figure 2.6.** Species classification map produced by PLS-DA and image texture parameters

## 2.4. Discussion

Whereas several studies have reported on the value of image texture in vegetation mapping (Franklin et al., 2000, Lottering et al., 2016, Lottering et al., 2020), its capability has not yet been fully explored in commercial forest species discrimination. Therefore, this study aimed to classify commercial forest species using image texture computed from a 0.5 m WorldView-2 pansharpened imagery using the PLS-DA algorithm. We then compared the image texture model with vegetation indices and spectral bands.

The results showed that although all models performed well in detecting commercial forest species, the PLS-DA image texture model performed better than the PLS-DA vegetation indices and the PLS-

DA spectral band models. This could be attributed to image texture simplifying vegetation canopy, variation in stand age, and the high spatial resolution of the WorldView-2 pansharpened image. Studies have found that image spatial resolution plays a significant role in texture analysis. Our results showing improved image texture performance is consistent with existing literature that reported improved performance of image texture over spectral reflectance data (Franklin et al., 2000, Moskal and Franklin, 2004, Sarker and Nichol, 2011, Dube et al., 2015, Lottering et al., 2019). For example, Nichol et al. (2010), found that image texture outperformed spectral reflectance data in estimating vegetation biomass in the Hong Kong Special Administrative Region in the southeast coast of China. Similarly, Dube et al. (2015), found that image texture outperformed spectral reflectance data in estimating plantation forest aboveground biomass in the Sappi Clan plantation forest in KwaZulu Natal, South Africa.

PLS-DA selected texture parameters predominantly from the red-edge, NIR1 and NIR2 bands of the WorldView-2 pan-sharpened image for discriminating commercial tree species. This was due to the structurally relevant information contained in these bands (Peerbhay et al., 2013b, Lottering et al., 2019, Lottering et al., 2020). The red-edge region is known to effectively determine vegetation health and classes (Barry et al., 2008, Eitel et al., 2011). For example, Champion et al. (2008), found that the red-edge region was the most valuable for discriminating invasive Giant reed from surrounding woody vegetation. In addition, Gong et al. (2003), showed the significant relationship between NIR and vegetation, thus increasing information available using image texture analysis. Moreover, co-occurrence image texture parameters were generally utilized for the development of the PLS-DA image texture model when compared to the occurrence image texture parameters. According to Rao et al. (2002), co-occurrence texture parameters are the most commonly adopted for remote sensing of vegetation. Gómez et al. (2012), noted that many studies have shown that co-occurrence provides better classification than occurrence texture measures. The results obtained in this study are similar to those of Yuan et al. (1991), who found that cooccurrence texture parameters better detected sugar maple decline than occurrence texture parameters. The most selected texture parameters for developing the PLS-DA model were homogeneity, correlation, and mean parameters. This finding is consistent with Lottering et al. (2020), who found that homogeneity and correlation were critical in detecting and mapping

invasive *Solanum mauritianum* and surrounding commercial forest species in KwaZulu-Natal South Africa.

Finally, the results showed that VIP generally selected the  $7 \times 7$  moving window for model development. The superior performance of the  $7 \times 7$  moving window can be attributed to the fact that larger window sizes can detect subtle textural changes and variance over larger areas within different stands (Dye et al., 2008), thus improving delineation and classification (Lottering et al., 2020). On the other hand, the inferior performance of the  $3 \times 3$  moving window can be attributed to the fact that smaller window sizes can exaggerate the difference within the moving window, thus increasing noise on the texture image (Lottering et al., 2020). This study found that image texture integrated with the PLS-DA algorithm displayed enhanced accuracy in discriminating commercial forest species. Hence, the total number of correctly classified samples were higher than the misclassified, providing a higher overall performance for all forest species.

In summary, results of this study proved that image texture computed from the 0.5 m WorldView2 pan-sharpened image integrated with the PLS-DA algorithm can be used to classify commercial forest species. This can be attributed to the high spatial resolution of the WorldView-2 image. This study paves a new way for adopting image texture in commercial forestry applications.

## **2.5. Conclusion**

Although the potential of image texture has been previously demonstrated, no study has investigated the potential of image texture in classifying commercial forest species. This study has therefore shown an integrated approach in classifying commercial forest species using image texture, vegetation indices and the PLS-DA algorithm. This study has revealed that:

- Image texture integrated with PLS-DA produced the highest overall accuracy, when compared to vegetation indices and spectral model in classifying commercial forest.
- Texture parameters selected by the PLS-DA were the homogeneity, correlation and mean, which were predominantly computed from the red-edge NIR1 and NIR2 bands.
- The  $7 \times 7$  moving window was most commonly selected by the PLS-DA model when compared to the  $3 \times 3$  and  $5 \times 5$  moving windows.

Overall, this study was the first to classify commercial forest using image texture and the PLS-DA algorithm. It showcases the significance of image texture in detecting and mapping commercial forest species.

## **2.6. Link to next chapter**

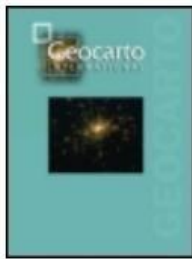
Although this study has showcased the significance of raw texture bands in significantly improving the detection and mapping of commercial forest species, this model can still only explain 77% in delineating these species. Therefore, the researchers decided to take it one step further in Chapter 3 to improve the model by testing the utility of texture combinations computed from fused WorldView-2 pan-sharpened imagery in discriminating commercial forest species.

## CHAPTER THREE

### UTILITY OF TEXTURE COMBINATIONS COMPUTED FROM FUSED WORLDVIEW-2 IMAGERY IN DISCRIMINATING COMMERCIAL FOREST SPECIES

---

This chapter is based on:



Geocarto International



ISSN: (Print) (Online) Journal homepage: <https://www.tandfonline.com/loi/tgei20>

#### Utility of texture combinations computed from fused WorldView-2 imagery in discriminating commercial Forest species

Bongokuhle Sibiya, Romano Lottering & John Odindi

To cite this article: Bongokuhle Sibiya, Romano Lottering & John Odindi (2021): Utility of texture combinations computed from fused WorldView-2 imagery in discriminating commercial Forest species, *Geocarto International*, DOI: [10.1080/10106049.2021.1952316](https://doi.org/10.1080/10106049.2021.1952316)

To link to this article: <https://doi.org/10.1080/10106049.2021.1952316>

Bongokuhle Sibiya, Romano Lottering & John Odindi, 2021. Utility of texture combinations computed from fused WorldView-2 imagery in discriminating commercial Forest species, *Geocarto International*, DOI: 10.1080/10106049.2021.1952316

## Abstract

Commercial forest species discrimination is valuable for optimal management of commercial forests. Therefore, second-order image texture combinations computed from a 0.5 m WorldView2 pan-sharpened image integrated with sparse partial least squares discriminant analysis (SPLSDA) and partial least squares discriminant analysis (PLS-DA) were used to discriminate commercial forest species. The findings show that the SPLS-DA model, which is characterised by concurrent variable selection and reduction of data dimensionality, produced an overall classification accuracy of 86%, with an allocation disagreement of 9 and a quantity disagreement of 5. Conversely, the PLS-DA model with variable importance in projection (VIP) produced an overall classification accuracy of 81%, with an allocation disagreement of 12 and a quantity disagreement of 7. Overall, this study demonstrates the value of second-order image texture combinations in discriminating commercial forest species and presents an opportunity for improved commercial forest species delineation.

**Keywords:** Texture combinations, Species discrimination, PLS-DA, SPLS-DA, WorldView-2

### 3.1. Introduction

Commercial forest plantations cover approximately 1.2 million hectares of South Africa's land mass (DAFF., 2012). These forests are predominantly located in the eastern and southern parts of the country with abundant rainfall and warmer temperatures (DAFF., 2012). Commercial forests contribute approximately 2% towards the country's gross domestic product and align with its environmental imperatives of reducing the effects of carbon dioxide and greenhouse gas emissions (Peerbhay et al., 2013a, Peerbhay et al., 2013b, Peerbhay et al., 2014, Dube et al., 2018, Mngadi et al., 2019). Hence, information on their distribution is crucial for making informed decisions that include monitoring ecosystems health, species management and harvest scheduling (Franklin et al., 2000, Peerbhay et al., 2013a, Peerbhay et al., 2013b, Mngadi et al., 2019). In addition, reliable discrimination of commercial forest species is valuable for, among others; terrestrial carbon accounting, climate change modelling, biodiversity assessments and fire hazard monitoring and control (Cho et al., 2010, Sarker and Nichol, 2011, Dube et al., 2015). In this regard, the establishment of reliable and timely forest discrimination approaches is necessary for achieving commercial and conservation related planning and monitoring.

Generally, conventional methods such as field surveys have been utilized for forest discrimination. However, the shortcoming of such approaches are widely documented in literature (Nichol et al., 2010, Peerbhay et al., 2013a, Peerbhay et al., 2013b, Hlatshwayo et al., 2019, Lottering et al., 2019, Lottering et al., 2020). Alternatively, remote sensing approaches have emerged as cost-effective means for monitoring and assessing vegetation, with reliable classification accuracies (Lottering and Mutanga, 2012, Barbosa et al., 2014, Dube et al., 2014, Bastin et al., 2014, Dube et al., 2015). Previous studies have generally utilized spectral data or vegetation indices to detect and map commercial forest species (Mutanga and Skidmore, 2004, Ingram et al., 2005, Lu, 2006, Godsmark, 2008, Mutanga et al., 2012, Dube et al., 2014, Sarker and Nichol, 2011, Nichol et al., 2010, Peerbhay et al., 2013a, Peerbhay et al., 2013b, Mngadi et al., 2019). Although the adoption of these approaches have produced reasonable classification accuracies, they are characterized by a range of limitations (Anderson et al., 1993, Dube et al., 2014, Dube et al., 2015, Hlatshwayo et al., 2019). For example, classification accuracies when using spectral vegetation indices are adversely affected by rapidly changing vegetation growth and canopy shadowing, while indices like NDVI saturate at dense biomass levels (Lu et al., 2002, Lu and Batistella, 2005, Mather and Koch, 2011, Sarker and Nichol, 2011, Hlatshwayo et al., 2019, Lottering et al., 2019, Lottering et al., 2020). Therefore, the adoption of alternative approaches that allow for improved delineation of vegetation structural characteristics are necessary (Fuchs et al., 2009, Nichol et al., 2010, Sarker and Nichol, 2011, Dube et al., 2015).

Image texture is useful in determining the spatial orientation of features and has previously been used for forestry management (Franklin et al., 2000, Sarker and Nichol, 2011, Dye et al., 2012, Hlatshwayo et al., 2019, Lottering et al., 2019, Lottering et al., 2020). In commercial forestry, it has been utilized to identify different forest stand structural characteristics that include density, age and leaf area index from medium-to-high spatial resolution images (Champion et al., 2008). The major strength of adopting image-texture is its ability to decompose and distinct heterogeneous forest canopies, including layered and closed canopies (Nichol et al., 2010, Sarker and Nichol, 2011, Dube et al., 2015, Lottering et al., 2020). Several studies have confirmed the role of texture analyses to improve classification accuracy, for instance, Lottering et al. (2020), recently used image texture to compare partial least squares (PLS) discriminant analysis and sparse PLS discriminant analysis to detect and map Bugweed (*Solanum mauritianum*) invasion in commercial forests of KwaZulu-Natal, South Africa, with overall accuracies of 67% and 77%,



respectively. In addition, Franklin et al. (2000), adopted texture analysis for the classification of forest species in New Brunswick and Canada; achieving a 5% and 12% improved classification accuracy in New Brunswick and Canada, respectively.

Whereas a number of studies e.g., Franklin et al. (2000), Moskal and Franklin (2004), Lottering et al. (2016) and Lottering et al. (2020), have explored the value of image texture in discriminating vegetation landscapes, our study focuses on the use of texture combinations in discriminating commercial forest species. Several studies, Hlatshwayo et al. (2019), Nichol et al. (2010), Dube et al. (2015), Lottering et al. (2019) have noted that texture combinations improve mapping accuracy over the use of single texture bands. For example, Lottering et al. (2019), used image texture combinations in detecting and mapping the Eucalyptus snout beetle (*Gonipterus scutellatus*) induced vegetation defoliation, while Hlatshwayo et al. (2019) explored the capability of image texture combinations in mapping aboveground biomass within a reforested landscape. Other studies including; Nichol et al. (2010), Sarker and Nichol (2011) and Dube et al. (2015) successfully used image texture combinations in mapping forest aboveground biomass, which plays a significant role in reducing background and atmospheric effects (Myneni et al., 1995, Wang et al., 2012).

While the use of image texture combinations has demonstrated great potential, its adoption requires an optimal feature extraction technique as textural combinations may be characterized by complex and redundant data (Lottering et al., 2020). Recently, the Partial Least Square Discriminant analysis (PLS-DA) has emerged as ideal when dealing with complex image texture combination data, as it can effectively reduce background effects and resolve tree species spectral similarities (Peerbhay et al., 2013b). Furthermore, PLS has the capability to store data into fewer PLS latent components (Peerbhay et al., 2013a, Sibanda et al., 2015), which preserve the most valuable texture combinations for analysis based on variable importance in the projection (VIP) (Sibanda et al., 2015, Peerbhay et al., 2013a, Peerbhay et al., 2013b, Lottering et al., 2020). Despite notable classification performance, PLS-DA has numerical limitation, especially when dealing with large datasets with too many correlated predictors (Lê Cao et al., 2008, Peerbhay et al., 2014). Therefore, there is a need to employ an innovative approach that is useful in examining dimensional and redundant image textural data using the improved Sparse Partial Least Square Discriminant Analysis (SPLS-DA) (Peerbhay et al., 2014, Lottering et al., 2020). However, there is a lack in

literature on studies that have examined the use of both PLS-DA and SPLS-DA in discriminating commercial forest species using texture combinations computed from multispectral image data. As a result, the aim of this study was to test the utility of texture combinations by comparing PLS-DA and SPLS-DA in discriminating commercial forest plantations using a WorldView-2 pansharpened image. The WorldView-2 pansharpened image was adopted due to its high spatial resolution, hence enhanced textural information for discriminating commercial forest species (Cheng and Chaapel, 2008, Dube et al., 2014, Mngadi et al., 2019, Lottering et al., 2019).

### **3.2. Material and methods**

#### ***3.2.1. The study area***

The study area is located in the Sappi Hodgson Estate in KwaZulu-Natal, South Africa (30°59'85" E; 29°19'03" S) (Figure 3.1). The area covers 6391 ha within the KwaZulu-Natal midlands mist belt grassland bioregion and receives 730 to 1590 mm annual rainfall, which is generally experienced during summer and mist conditions during winter. The landscape is classified as rolling and hilly, with an elevation ranging from 1030 to 1590 m above sea level. The primary tree stands in the area are Pine (*P. Patula*), Eucalyptus (*E. Grandis* and *E. Dunnii*) and Acacia (*A. Mearnsii*).

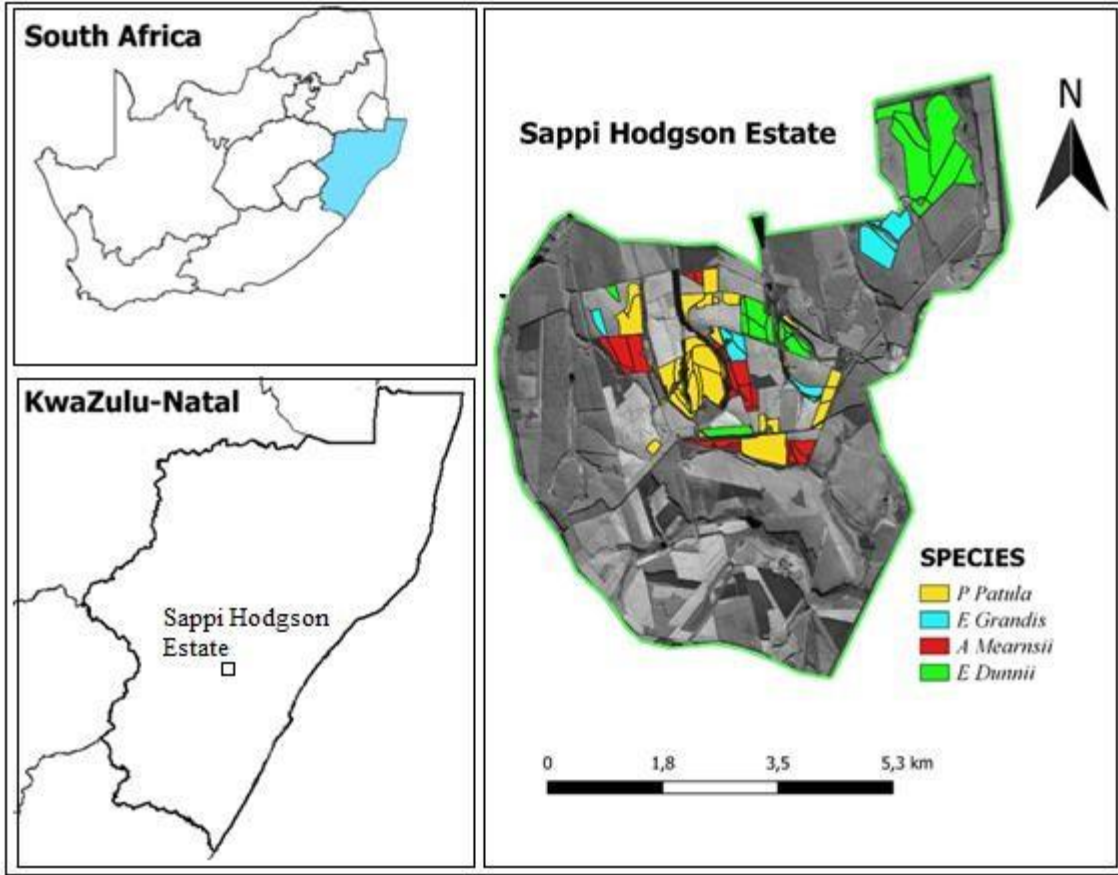


**Figure 3.1.** Location of the study area within KwaZulu-Natal Province, South Africa

### 3.2.2. Image acquisition

A 0.5 m WorldView-2 pan-sharpened image obtained under cloudless conditions on the 20th of September 2012 was used in this study. The WorldView-2 pan-sharpened image is comprised of eight wavebands (Table 3.1). Using ENVI 4.7 software, the image was atmospherically corrected to the top-of-atmosphere reflectance (ToAR). As a function of the WorldView-2 pan-sharpened bands, the shape of the solar curve determined the shape of the top-of-atmosphere spectral radiance. The ToAR for the WorldView-2 pan-sharpened image is given by:

$$p_{\lambda_{\text{Pixel}}, \text{Band}} = \frac{L_{\lambda_{\text{Pixel}}, \text{Band}} \cdot d_{\text{ES}}^2 \cdot \pi}{E_{\text{sun}, \lambda_{\text{Band}}} \cdot \cos(\theta_s)} \quad (1)$$

Where  $L_{\lambda_{\text{Pixel}}, \text{Band}}$  represents the ToAR band averaged respectral radiance,  $d_{\text{ES}}$  is the Earth-Sun distance during the acquisition of the WorldView-2 pan-sharpened image,  $E_{\text{sun}, \lambda_{\text{Band}}}$  represents the band average solar spectral irradiance normal to the surface that is illuminated and  $\theta_s$  represents that solar zenith angle during the acquisition of the WorldView-2 pan-sharpened image (Omar,

2010). The image was then geo- and ortho - rectified using twenty-five evenly spread ground control points. A geo-rectification root means square error (RMSE) of less than 0.5 m was obtained, and the image projected to Universal Transverse Mercator projection and the World Geodetic System 84 datum.

**Table 3.1:** Characteristics of the WorldView-2 pan-sharpened bands

Band	Range (nm)	Spatial resolution (m)
Coastal blue	400-450	0.5
Blue	450-510	0.5
Green	510-580	0.5
Yellow	585-625	0.5
Red	630-690	0.5
Red edge	705-745	0.5
Near-IR1	770-895	0.5
Near-IR2	860-1040	0.5

### 3.2.3. Field data collection

Six forest stands per species (*A. Mearnsii*, *E. Dunnii*, *E. Grandis* and *P. Patula*) were selected randomly within the study area and field surveys conducted to verify the status of the selected stands. The Hawth's tool in QGIS Desktop 3.14.16 was used to create  $30 \times 30$  m random plots over the study area using an existing WorldView-2 image. To ensure that the sample sizes of each species was balanced and statistically representative, each stand was sub-sampled to ensure that the sample plots were equally distributed (Table 3.2). The final dataset consisted of 240 samples plots with 70% ( $n = 168$ ) used as the training dataset and 30% of the sample plots ( $n = 72$ ) were used as the test dataset. According to Peerbhay et al. (2013a) and Peerbhay et al. (2013b) a balanced number of class sample plots for training and testing data is critical for PLS-DA optimization. Furthermore, the RStudio statistical software package version 3.1.3 (Team, 2013) was used to run the data to guarantee that the number of samples in the test and training datasets for each species were approximately similar (Table 3.2).

**Table 3.2:** Sample size of each species surveyed (n = 240)

Species	Number of stands	No. of samples	Total sample points
<i>A. mearnsii</i>	6	10	60
<i>E. dunnii</i>	6	10	60
<i>E. grandis</i>	6	10	60
<i>P. patula</i>	6	10	60

#### **3.2.4. Image Texture**

Image texture refers to local variance within an image in relation to properties of neighbourhood pixels (Lottering et al., 2019). This method could be useful in discriminating commercial forest species as species type, crown closure or stem density could result in a variation in image texture (Franklin, 2001). Therefore, by utilizing texture parameters, it is possible to determine the spatial distribution and image tone variability (Moskal and Franklin, 2004).

A range of texture analysis approaches have been developed to extract image features from remotely sensed imagery (Li et al., 2015). These approaches can be grouped into first-order and second-order texture parameters (Lottering and Mutanga, 2012). The first-order texture is determined based on pixel intensities of the histogram within a processing window (Hlatshwayo et al., 2019, Chetty, 2020) and is independent of the adjacent pixels (St-Louis et al., 2006). The second-order texture parameters rely on neighbourhood pixels grey tone matrix to compute texture (Sarker and Nichol, 2011). A number of studies have established that the performance of second-order texture parameters is superior to first-order texture parameters within forest environments (Yuan et al., 1991, Moskal and Franklin, 2004, Sarker and Nichol, 2011, Lottering and Mutanga, 2012, Dube et al., 2015, Lottering et al., 2020). Hence, this study adopted second-order texture parameters (Table 3.3) computed from a WorldView-2 pan-sharpened image to discriminate commercial forest species, using a shift of  $x = 1$ ,  $y = 1$  and  $\theta = 45^\circ$ . The angle adopted was found to be suitable in calculating image texture parameters to classify commercial forestry.

**Table 3.3:** Filters for the second-order texture parameters

Parameter	Formula	Description
Contrast	$\sum_{i,j=0}^{N-1} P_{i,j} (i - j)^2$	Determines the level of local variation within a window (Yuan et al., 1991, Haralick et al., 1973).
Correlation	$\sum_{i,j=0}^{N-1} P_{i,j} \left[ \frac{(i - \mu_i)(i - \mu_j)}{\sqrt{(\sigma_i^2)(\sigma_j^2)}} \right]$	Estimates the grey-level linear dependency in an image (Lottering et al., 2019, Haralick et al., 1973).
Dissimilarity	$\sum_{i,j=0}^{N-1} P_{i,j}  i - j $	Establishes local variation (Rubner et al., 2001, Haralick et al., 1973).
Entropy	$\sum_{i,j=0}^{N-1} P_{i,j} (-\ln P_{i,j})$	Measures statistical uncertainty (Yuan et al., 1991, Haralick et al., 1973).
Homogeneity	$\sum_{i,j=0}^{N-1} \frac{P_{i,j}}{1 + (i - j)^2}$	Determines smoothness of texture (Hlatshwayo et al., 2019, Haralick et al., 1973).
Mean	$\mu_i = \sum_{i,j=0}^{N-1} i(P_{i,j})$ $\mu_j = \sum_{i,j=0}^{N-1} j(P_{i,j})$	Mean grey-level within a small neighborhood (Materka and Strzelecki, 1998, Haralick et al., 1973).
Second moment	$\sum_{i,j=0}^{N-1} P_{i,j}^2$	Indicators local homogeneity (Yuan et al., 1991, Haralick et al., 1973).
Variance	$\sigma_i^2 = \sum_{i,j=0}^{N-1} P_{i,j} (i - \mu_i)^2$ $\sigma_j^2 = \sum_{i,j=0}^{N-1} P_{i,j} (i - \mu_j)^2$	Variability of the spectral response of pixels (Materka and Strzelecki, 1998, Haralick et al., 1973).

Where  $\mu_i$ ,  $\mu_j$ ,  $\sigma_i$  and  $\sigma_j$  represent means and std. deviations of marginal distributions associated with  $P(i, j)$  which is the normalised co-occurrence matrix such that  $\sum_{i,j=0}^{N-1} (P(i, j)) = 1$

Texture parameters were computed from the WorldView-2 pan-sharpened image using a  $7 \times 7$  moving window size and the mean value of the sample plots (240) were extracted using zonal statistics in QGIS Desktop 3.14.16. Texture combinations were subsequently computed using two texture parameters that were generated from the same band. These texture combinations were generated using equation (2).

$$\text{Image texture} = \frac{T_1}{T_2} \quad (2)$$

Where  $T_1$  and  $T_2$  are texture parameters.

### 3.2.5. Statistical analysis

#### 3.2.5.1. Partial least squares discriminant analysis (PLS-DA)

The Partial least squares (PLS) is known as Partial least squares discriminant analysis (PLS-DA) when used for classification purposes, however, in general, it is referred to as a parametric linear method (Peerbhay et al., 2013b). For PLS-DA to create a predictive model, it is dependent on the traditional partial least squares' regression approach. Furthermore, PLS regression seeks to reduce data dimensionality, where there is a link between the response variable (Y) and the predictor variables (X). The response variable (i.e., commercial forest species) is binary and expresses class membership in the case of PLS-DA (Castillo-Santiago et al., 2010, Galtier et al., 2011, Peerbhay et al., 2013a, Peerbhay et al., 2013b, Peerbhay et al., 2014). Partial least squares aim to identify a few eigenvectors of spectral matrices to generate scores that explain both the variance of the texture data and the high correlation with the response variables (Li et al., 2007, Li et al., 2008, Wolter et al., 2008): The approach is executed using the following expression:

$$\mathbf{X} = \mathbf{TP}^T + \mathbf{E} \quad (3)$$

$$\mathbf{Y} = \mathbf{UQ}^T + \mathbf{F} \quad (4)$$

where X characterizes the matrix of the image texture combinations, Y characterizes the matrix of the commercial forest species ( $n = 240$ ), T is a factor score matrix, U is the scores for Y, Q is the Y loadings, P is the X loadings, E is the residual for X or a noise term, and F is the residuals for Y (Peerbhay et al., 2013a, Peerbhay et al., 2013b, Lottering et al., 2020).

#### 3.2.5.2. Variable importance in the projection

PLS-DA does not have the ability to select the most important texture combinations and is dependent on the variable importance in the projection for this (VIP) (Peerbhay et al., 2013a). The VIP produces a score as a measure of the most important texture combinations and is defined as follows:

$$VIP_k = \sqrt{K \sum_{a=1}^A [(q_a^2 t_a^T t_a) (W_{ak} / \|W_k\|^2)] / \sum_{a=1}^A (q_a^2 t_a^T T_a)} \quad (5)$$

Peerbhay et al. (2013a), defines VIP as a technique that generates a ranked score of bands within the data set, where,  $VIP_k$  represents the importance of the  $k$ 'th texture combination relating to the PLS-DA model,  $w_{ak}$  represents the consistent loading weight of the  $k$ 'th texture combination in the  $a$ 'th PLS-DA component,  $t_a$ ,  $w_a$ , and  $q_a$  are the  $a$ 'th column vectors and  $K$  is the total number of texture combinations (Peerbhay et al., 2013b, Lottering et al., 2020). The important texture combinations can be identified by VIP scores above 1 as the average of the squared VIP scores equals to 1. In our study, a new PLS-DA model was generated from the selected VIP texture combinations, which were then used to map the commercial forest species. The PLS-DA model optimization, discriminant analysis and VIP were executed in RStudio statistical software package version 3.1.3 (Team, 2013).

### 3.2.5.3. Sparse partial least squares discriminant analysis (SPLS-DA)

In this study, a sparse version of the PLS for discrimination purposes, which is a natural extension of PLS-DA (Lê Cao et al., 2008) was utilized. Although PLS was developed for regression (Lê Cao et al., 2008), it is also useful for classification purposes. Utilizing this approach for discriminating commercial forest plantations is useful, especially when examining high dimensional and redundant image texture combination data, which might be challenging for PLS-DA. In the discrimination process, SPLS-DA recruits a scarcity solution that concurrently selects variables and reduces dimensionality, where irrelevant and noisy variables are scored a zero value by imposing L1 penalty (Chun and Keleş, 2010). As a result, reducing the contribution of irrelevant variables in the modelling process (Lottering et al., 2020). In addition, Peerbhay et al. (2014), notes that the latent components are used to explain the optimal discrimination within classes by adopting few useful variables (i.e., non-zero variables) and maximize the covariance between the predictor and response variables. Variable class membership is then assigned by coding the reference cell response matrix ( $Y$ ) with dummy variables (Chun and Keleş, 2010).  $Y$  is assumed to be one of the classes ( $G + 1$ ) indicated by 0, 1, ...,  $G$ . The recoded response matrix is then defined as  $n \times (G + 1)$  matrix with:

$$y_{i,(g+1)}^* = I(y_i = g) \quad (6)$$

where  $i = 1 \dots, n$ ;  $g = 0; 1 \dots, G$ , and  $I$  is an indicator function of event ( $A$ ). After constructing latent components, since the number of latent components ( $K$ ) is generally smaller than  $n$ , the last step required in SPLS-DA is to fit a classifier. Therefore, linear classifiers are generally used for this



purpose (Chun and Keleş, 2010). In this study, we used the “splsga” function in R statistical package version 3.1.3 (Team, 2013) to run the SPLS-DA algorithm.

#### *3.2.5.4. Optimization of PLS-DA and SPLS-DA models*

To develop the PLS-DA model, a tenfold cross-validation (CV) approach was utilized to identify the number of components required. The number of components were systematically introduced to the model and the CV error was then established (Menze et al., 2009). This process was repeated on the training dataset until the addition of more components did not improve the performance of the model. Once optimised, the PLS-DA model was then used to classify the training dataset. For the SPLS-DA model, two parameters were utilized for model optimization; (1) “k” the number of latent components, which is an integer value that is dependent on the size of the sample and the number of explanatory variables, and (2) “eta” a sparsity thresholding parameter that ranges between 0 and 1 (Chun and Keleş, 2010). In this process, optimal latent components retain the most effective texture combinations, while un-important texture combinations are assigned a zero probability. Ultimately, the optimized SPLS-DA model was used to classify the image. PLS-DA and SPLS-DA model optimization were executed in the RStudio statistical software package version 3.1.3 (Team, 2013).

#### *3.2.6. Accuracy assessment*

The entire dataset (240) was divided into training (70%) test data (30%), with the latter dataset being used to create the confusion matrix. To account for variations in accuracy resulting from divergent training and testing compositions, the process was run using 100 iterations. Due to Kappa analysis being criticised for comparing observed and predictable accuracy (Fassnacht et al., 2014), the allocation and quantity disagreement was used to determine the error matrix. In the quantity disagreement process, the number of samples for a specific tree species for the training dataset is measured by the allocation disagreement, whereas the number of trees samples in the training dataset that differ from the samples in the test dataset are calculated by the quantity disagreement (Atkinson et al., 2013). As a result, both disagreements are used in the error matrix.

Figure 3.2 shows a flowchart of the research methodology for this study.

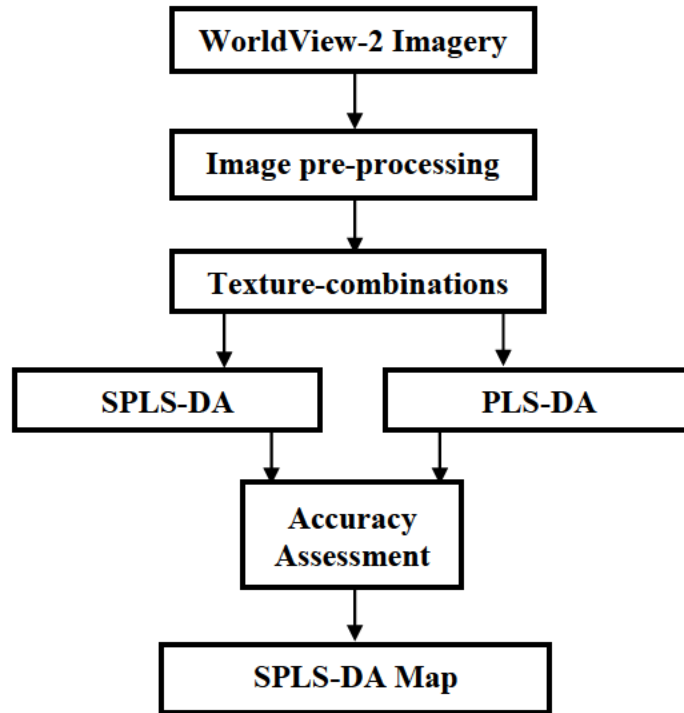


**Figure 3.2.** Summary of workflow followed in this study.

### 3.3. Results

#### 3.3.1. Optimizing the PLS-DA model

Figure 3.3 illustrates the reduction in CV error from the 1st (45%) component to using 10 components (21%), which was based on a tenfold cross-validation method using the training dataset ( $n = 168$ ). The figure shows that 8 components generated the lowest error (17%), therefore was adopted to generate the PLS-DA model and calculate VIP scores for each texture combination.

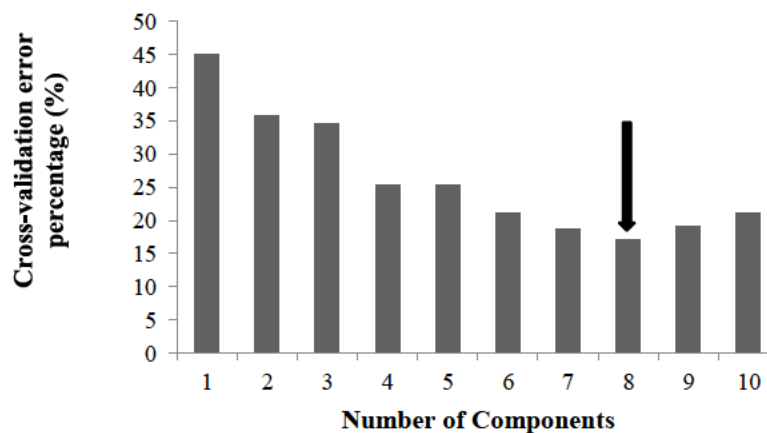


**Figure 3.3.** Testing the discriminatory capability of individual PLS-DA components using texture combinations. The black arrow shows the component with the lowest error.

### 3.3.2. *PLS-DA and VIP*

VIP selected 75 significant image texture combinations for the PLS-DA model. The results show that the model generated an overall accuracy of 81%, with an allocation disagreement of 12 and a quantity disagreement of 7. Accuracies for individual species users and producers ranged from 73% to 88% (Table 3.4). Figure 3.4 shows the variation in accuracy based on 100 iterations for the training and validation dataset split. A mean overall classification accuracy of 79.6% with a standard deviation of 2.29 was achieved.

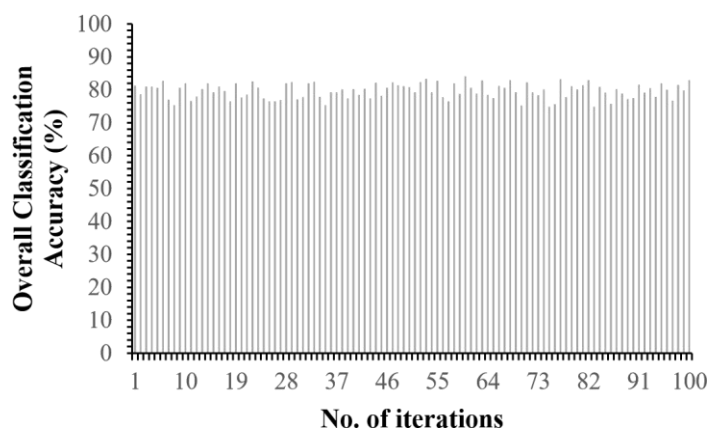


**Figure 3.4.** PLS-DA classification accuracies produced based on 100 iterations for splitting the training and validation data.

### 3.3.3. *SPLS-DA model optimization*

Figure 3.5 indicates the significance of each SPLS-DA component using a tenfold cross validation method, which was based on the training dataset ( $n = 168$ ). The initial component produced a CV error of 35%, which was later reduced to 16% by using 10 components. The most significant component, however, was achieved by using 7 components which produced the lowest CV error rate. These components were subsequently used to develop the SPLS-DA model. In addition, an “ $\eta$ ” of 0.3 and “ $k$ ” of 6 were optimum parameters for developing the SPLS-DA model.

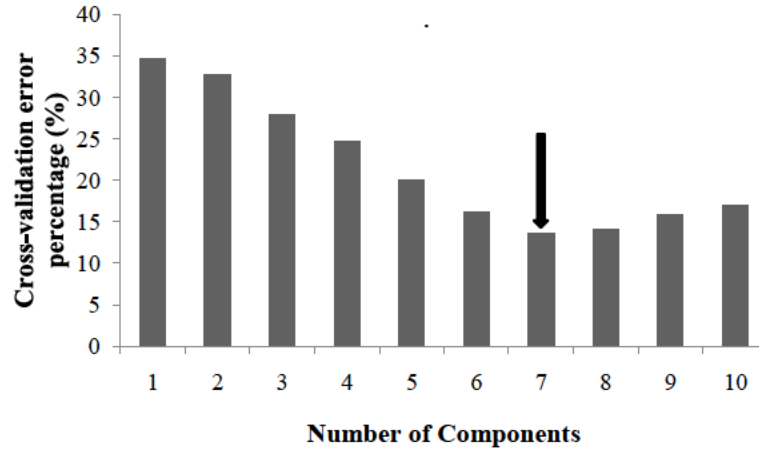


**Figure 3.5.** Testing the discriminatory capability of individual SPLS-DA components using texture combinations. The black arrow shows the component with the lowest error.

The results show that the use of image texture combinations with 7 components generated an overall accuracy of 86%, with an allocation disagreement of 9 and a quantity disagreement of 5.

The user's and producer's accuracies for each species ranged from 77% to 98% (Table 3.4). Figure 3.6 shows the variation in classification accuracy generated by SPLS-DA model based on 100 iterations for splitting the training and validation data. A mean overall classification accuracy of 86% with a standard deviation of 2.49 was achieved.

**Table 3.4:** Classification results for discriminating commercial forest species using the SPLSDA and PLS-DA models.

Accuracy measurements		Models	
		SPLS-DA	PLS-DA
<i>A. mearnsii</i>	User's accuracy	85	80
	Producer's accuracy	93	87
<i>E. dunnii</i>	User's accuracy	84	78
	Producer's accuracy	78	77
<i>E. grandis</i>	User's accuracy	82	78
	Producer's accuracy	77	73
<i>P. patula</i>	User's accuracy	98	88
	Producer's accuracy	91	88
Overall accuracy		86%	81%
Allocation disagreement and Quantity disagreement		9 and 5	12 and 7

A McNemar's test was then run to establish whether there was a statistically significant improvement in the overall classification accuracy of SPLS-DA over PLS-DA. The null hypothesis  $H_0$ : there was no significant difference ( $p > 0.05$ ) vs the alternate hypothesis  $H_a$ : there was a

significant difference ( $p < 0.05$ ). We subsequently rejected the null hypothesis as there was a significant difference in the overall classification accuracy ( $p < 0.05$ ).

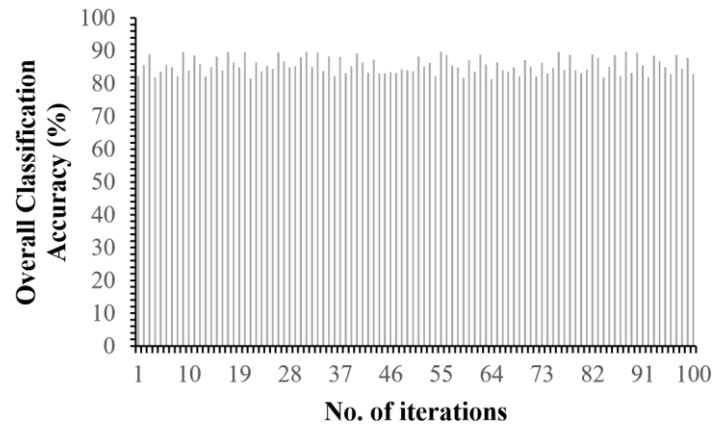


**Figure 3.6.** SPLS-DA classification accuracies produced based on 100 iterations for splitting the training and validation data.

### ***3.3.4. Testing and Applying the principal component analysis (PCA) to discriminate commercial forest species for comparative purposes***

The principal component analysis (PCA) is a method that is similar to PLS in terms of reducing data dimensionality, however it is an unsupervised technique (Arowolo et al., 2021). For comparative purposes, PCA was used to discriminate commercial forest species using the same dataset. Results showed that SPLS-DA, with 86% overall classification accuracy was higher than PCA with 78% overall classification accuracy.

### ***3.3.5. Frequency of selected significant variables for the SPLS-DA model***

Since the SPLS-DA model outcompeted the PLS-DA model, we only highlighted the top 10 combinations used to develop the SPLS-DA model (Table 3.5). SPLS-DA selected 58 significant image texture combinations to effectively discriminate commercial forest species. Furthermore, the WorldView-2 pan-sharpened texture combinations derived from the Mean/Second Moment, Homogeneity/Second Moment, and Entropy/Second Moment appeared more times in the top 10 selected parameters. In addition, these texture combinations were generally computed from the red, red edge and NIR bands.

**Table 3.5:** Top 10 selected image texture combinations for the SPLS-DA model

Rank	SPLS-DA		
	Band	Moving Window	Texture combination
1	Red edge	7 x 7	Mean/Second Moment
2	NIR 1	7 x 7	Correlation/Second Moment
3	Red	7 x 7	Dissimilarity/Mean
4	NIR 2	7 x 7	Homogeneity/Second Moment
5	Green	7 x 7	Mean/Second Moment
6	NIR 1	7 x 7	Entropy/Second Moment
7	Red Edge	7 x 7	Homogeneity/Second Moment
8	Red	7 x 7	Homogeneity/Second Moment
9	NIR 2	7 x 7	Second Moment/Second Moment
10	NIR 1	7 x 7	Entropy/Second Moment

### 3.3.6. Mapping the distribution of commercial forest species using SPLS-DA

Since the SPLS-DA model produced the highest overall accuracy, we then used it to map the spatial distribution of commercial forest species. Figure 3.7 shows the spatial distribution of commercial forest species over the study area. This distribution map, which covers 1156 ha of the study area, illustrates the ability of texture combinations integrated with the SPLS-DA model to effectively map the distribution of commercial forest species. This output is vital for making informed decisions that may include monitoring forest health, species management and harvest scheduling. The map is comparable to that of the WorldView-2 image, with *P. patula* being the dominant tree species. *E. dunni* and *E. grandis* were least correctly mapped species due to both species belonging to the same genus, respectively.

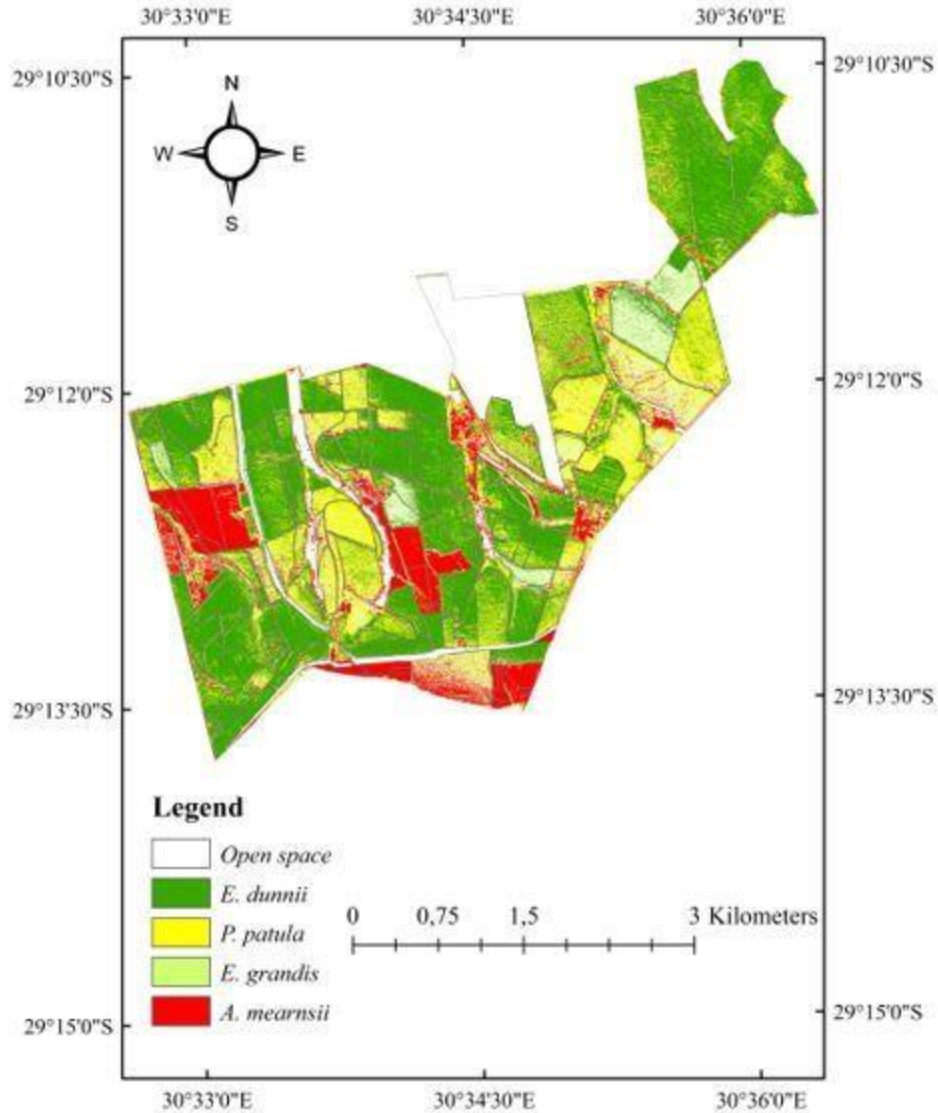


**Figure 3.7.** Species classification map produced by SPLS-DA model and image texture combinations

### 3.4. Discussion

To effectively manage commercial forests, it is important to accurately and reliably map their species. However, conventional methods such as field surveys have proven to be spatially restrictive. Hence, our study explored the value of remote sensing approaches to effectively discriminate commercial forest plantation using image texture combinations computed from a 0.5 m WorldView2 pan-sharpened image. We also investigated the utility of SPLS-DA and PLSDA in discriminating commercial forest plantations.

The findings in this study demonstrated the potential of image texture combinations computed from a WorldView-2 pan-sharpened image in conjunction with SPLS-DA and PLS-DA to discriminate commercial forest species. While both models successfully discriminated commercial forest species, the SPLS-DA was more effective. The lower overall classification accuracy of the PLS-DA model suggests that it may not be as effective in dealing with high data dimensionality (Lottering et al., 2020). This finding is similar to (Chun and Keleş, 2010), who noted that SPLSDA outperformed the PLS-DA model. Furthermore, PLS-DA was unable to effectively deal with texture similarities, especially between species of the same genus, hence lowered its overall model performance.

Incorporating SPLS-DA with second-order texture combinations and 7 components yielded an overall classification accuracy of 86%. However, our results differ from the findings of Lottering et al. (2020) and Peerbhay et al. (2014), who found an overall classification accuracy of 80% when discriminating forest species and 77% overall accuracy when mapping *Solanum mauritianum* in commercial forest plantations, respectively. The lower classification accuracy between these studies could be due to Peerbhay et al. (2014) using spectral data to delineate species, while Lottering et al. (2020), used single texture parameters. Our study takes one step further by utilizing texture combinations and our findings are consistent with a number of studies (Nichol et al., 2010, Dube et al., 2015, Hlatshwayo et al., 2019, Lottering et al., 2019) that have established that image texture combinations simplifies vegetation canopy structure, making it easier to discriminate between commercial forest species.

Furthermore, Mean/Second Moment, Homogeneity/Second Moment and Entropy/Second Moment played a significant role in developing the SPLS-DA model using the 7×7 moving window. This could be due to these texture combinations corresponding to the high spatial resolution of the WorldView-2 pan-sharpened image. These texture parameters have also produced significant results in several other studies. (Salas et al., 2016), for instance, established that homogeneity and second moment played an important role in mapping summer vegetation in the eastern Pamir Mountains, Tajikistan. In another study, Lottering et al. (2020), found that homogeneity and second moment were integral texture parameters in developing the SPLS-DA model for detecting and mapping *Solanum mauritianum* and surrounding commercial forest species. In addition, the SPLS-DA model generally selected texture parameters that were computed from the red, red-edge



and NIR bands of the WorldView-2 pan-sharpened image, which can be attributed to the value of these bands in vegetation mapping as noted by other studies (e.g. (Gebreslasie et al., 2011, Hlatshwayo et al., 2019, Lottering et al., 2019)).

For example, the red edge region is known to differentiate tree species due to its sensitivity to plant pigmentation within the leaf tissue (Peerbhay et al., 2013b). Fernandes et al. (2013), noted the value of this region in discriminating invasive species from surrounding woody vegetation, while Gong et al. (2003), demonstrated the co-relationship between NIR and vegetation.

This study established that image texture combinations generated from a 0.5 m WorldView-2 pansharpened image using the SPLS-DA algorithm successfully discriminated commercial forest species. Hence, the findings of this study provide a basis for mapping larger spatial extents using readily and freely available remotely sensed datasets such as Sentinel-2 or Landsat 8.

### **3.5. Conclusion**

This study adopted an integrated approach in discriminating commercial forest species. Using second-order image texture parameters in concert with a  $7 \times 7$  moving window and the PLS-DA and SPLS-DA algorithms, these are the conclusions made:

- An integration of the PLS-DA algorithm with second-order image texture combinations generated an overall classification accuracy of 81%, with an allocation disagreement of 12 and a quantity disagreement of 7.
- An integration of the SPLS-DA algorithm second-order image texture combinations generated an overall classification accuracy of 86%, with an allocation disagreement of 9 and a quantity disagreement of 5.
- The SPLS-DA model, with simultaneous variable selection and dimension reduction, was more superior than the PLS-DA model in discriminating commercial forest species.

In essence, this study pioneers the use of second-order image texture combinations integrated with the SPLS-DA algorithm to delineate commercial forest species. These findings are valuable in understanding commercial forest species distribution, which is useful for forest management.

## CHAPTER FOUR

### 4. SYNTHESIS

---

#### 4.1. Introduction

Accurate and precise information on a forest landscape is crucial for effective management and monitoring of commercial forest plantations. In addition to commercial value, plantation forests also play a crucial role in carbon assimilation and climate change mitigation, among others (Mngadi et al., 2019). Hence, information relating to the distribution, composition, and productivity of a commercial forest is critical for understanding the dynamics of commercial forest plantations (Peerbhay et al., 2013b, Peerbhay et al., 2014, Lottering et al., 2016). Moreover, discriminating commercial forest species is required for, among others; conservation planning, biodiversity assessments, site management practices, harvest scheduling, and fire hazard monitoring and control (Dube et al., 2018). Therefore, achieving these demands require effective and efficient approaches for forest discrimination that can improve the planning, monitoring and conservation efforts. Previous studies have mainly relied on surveys, whose shortcomings are widely documented in literature (Sarker and Nichol, 2011, Peerbhay et al., 2014, Mngadi et al., 2019). However, in recent decades, remote sensing has emerged as a cost-effective alternative for monitoring and assessing vegetation whilst producing very high classification accuracies. Generally, previous studies adopting remote sensing approaches have utilized spectral vegetation indices to detect and map commercial forest species, with less focus on spatial landscape characteristics (Hlatshwayo et al., 2019, Lottering et al., 2019). Therefore, the main focus of this study was to discriminate commercial forest species using image texture computed from a 0.5 m WorldView-2 pan-sharpened image in KwaZulu-Natal, South Africa. The aim and objectives of the study are reviewed against the research undertaken throughout this thesis:

#### 4.2. Aim and objectives reviewed

##### 4.2.1. Aim

The main aim of this study was to discriminate commercial forest species, using image texture computed from a 0.5m WorldView-2 pan-sharpened image.

#### 4.2.2. Objectives reviewed

In this study two objectives were set out to meet the aim aforementioned. This section will review how close the study came to meeting these objectives.

##### **□ Discriminating commercial forest species using image texture computed from a WorldView-2 pan-sharpened image and Partial Least Squares Discriminate Analysis**

Discriminating forest species using spectral data or vegetation indices has remained a challenge, particularly when mapping highly dense canopies, because of saturation and the mixed pixel problem. Therefore, the use of image texture offers a viable alternative for forest species discrimination and mapping. Based on the findings in this study, the image texture model outcompeted both the vegetation indices model and raw spectral bands model in discriminating commercial forest species. This study acknowledges the approximate 8% difference between image texture and vegetation indices and 13% between texture and spectral data. Hence, it can be concluded that image texture is superior to vegetation indices and spectral bands in discriminating commercial forest species. Specifically, the valuable parameters selected in classifying commercial forest species by the PLS-DA were the homogeneity, correlation and mean, which were predominantly computed from the red edge and infrared bands. In addition, the 7x7 moving window was commonly selected by the PLS-DA model when compared to the 3x3 and 5x5 moving windows. In conclusion, this objective demonstrated the ability of image texture in discriminating commercial forest species.

##### **□ To explore the Utility of texture combinations computed from fused WorldView-2 imagery in discriminating commercial Forest species**

This objective extended on the previous objective, by exploring the utility of the image texture combinations in conjunction with PLS-DA and SPLS-DA. Based on the results, the utility of the image texture combinations showed a significant improvement when mapping and discriminating commercial forests species. The results indicated that SPLS-DA successfully performed simultaneous variable selection and dimension reduction, outcompeting PLS-DA model in conjunction with VIP. Overall, our study demonstrated the potential of image texture combinations in discriminating commercial forest species. With the application of SPLS-DA

algorithm, results in this objective demonstrated the value of exploiting full capabilities of image texture combinations for improved forest species discrimination and mapping.

#### **4.3. Conclusions**

The major aim of this study was to discriminate commercial forest species using image texture computed from a WorldView-2 pan-sharpened image in KwaZulu-Natal, South Africa. The findings of this study concluded that image texture is an important and powerful tool in discriminating commercial forest species. In addition, the utility of texture combinations showed a great improvement when compared to raw texture parameters. The improved performance of the overall models indicated their capability in long-term assessments of commercial forest plantations. This conclusion is consolidated based on the observations achieved throughout this thesis and respond to the key research questions posed in Chapter One:

- **Can image texture and PLS-DA detect and map commercial forest species?**

This study has decisively shown the ability of image texture parameters with PLS-DA to detect and map commercial forest species. Based on the results, the PLS-DA image texture model successfully discriminated commercial tree species outperforming both the PLS-DA vegetation indices and the PLS-DA spectral band models. This was due to image texture simplifying vegetation canopy, variation in stand age, and the high spatial resolution of the WorldView-2 pansharpened image. In addition, the outcome may also be due to the capability of PLS-DA to decrease background effects and ability to overcome the issues of textural similarities between plantations. Hence, PLS-DA image texture created platform for detecting and mapping commercial forest species.

- **Does image texture combinations in conjunction with SPLS-DA effectively discriminate forest species?**

The utilization of texture combinations in the present study showcased the capability of texture combinations to adequately detect and map forest species when compared to raw image texture parameters. The outstanding achievement from texture combinations is due to bands combinations and the high spatial resolution of the WorldView-2 pan-sharpened image.

Texture combinations produced an outstanding performance due to their ability to deal with topographic effects and errors related with angle from the sensor and sunlight radiance. This makes texture combinations the number one candidate for discriminating commercial tree species in contrast to spectral reflectance and vegetation indices that lacks the ability to deal with complex vegetation structures.

In addition, the outstanding performance displayed by texture combination is related to integrating texture combinations with SPLS-DA. This is because SPLS-DA was able to delineate commercial forest species in areas where the PLS-DA model was unable. The outstanding performance is due to the fact that SPLS-DA was able to overcome issues related to high data dimensionality, which was not effectively dealt with by the PLS-DA algorithm. Therefore, combining SPLS-DA with second-order image texture combination and the 7x7 moving window offered improved and invaluable information that improved the overall classification outputs.

#### **4.4. The future**

Image texture offers new data sources critical for commercial forest species discrimination and mapping. The findings of this study present an insight on the utility of image texture in forest species discrimination and mapping. However, this study recommends that:

- This approach could be applied to large areas by using other remotely sensed images such as Landsat 8 OLI or Sentinel-2, which are freely available to test its regional classification potential.
- Image textures need to be further tested, in conjunction with new Textural indicators and Variogram analysis for the improved regional forest species discrimination and mapping.

## References

- Adelabu, S., Mutanga, O., Adam, E.E. and Cho, M.A., 2013. Exploiting machine learning algorithms for tree species classification in a semiarid woodland using RapidEye image. *Journal of Applied Remote Sensing*, 7, 073480.
- Ahamed, T., Tian, L., Zhang, Y., Ting, K. J. B. & Bioenergy 2011. A review of remote sensing methods for biomass feedstock production. *Biomass and bioenergy*, 35, 2455-2469.
- Anderson, G.L., Hanson, J.D. and Haas, R.H., 1993. Evaluating Landsat Thematic Mapper derived vegetation indices for estimating above-ground biomass on semiarid rangelands. *Remote sensing of environment*, 45, 165-175.
- Arowolo, M.O., Adebisi, M.O., Aremu, C. and Adebisi, A.A., 2021. A survey of dimension reduction and classification methods for RNA-Seq data on malaria vector. *Journal of Big Data*, 8, 1-17.
- Atkinson, J.T., Ismail, R. and Robertson, M., 2013. Mapping bugweed (*solanum mauritianum*) infestations in *pinus patula* plantations using hyperspectral imagery and support vector machines. *IEEE Journal of Selected Topics in Applied Earth Observations and Remote Sensing*, 7, 17-28.
- Bannari, A., Asalhi, H. & Teillet, P. M. 2002. Transformed difference vegetation index (TDVI) for vegetation cover mapping. *IEEE International geoscience and remote sensing symposium*, IEEE, 3053-3055.
- Barbosa, J.M., Melendez-Pastor, I., Navarro-Pedreño, J. and Bitencourt, M.D., 2014. Remotely sensed biomass over steep slopes: An evaluation among successional stands of the Atlantic Forest, Brazil. *ISPRS Journal of Photogrammetry and Remote Sensing*, 88, 91-100.
- Barry, K.M., Stone, C. and Mohammed, C.L., 2008. Crown-scale evaluation of spectral indices for defoliated and discoloured eucalypts. *International journal of remote sensing*, 29, 47-69.
- Bastin, J.F., Barbier, N., Couteron, P., Adams, B., Shapiro, A., Bogaert, J. and De Cannière, C., 2014. Aboveground biomass mapping of African forest mosaics using canopy texture analysis: toward a regional approach. *Ecological Applications*, 24, 1984-2001.
- Castillo-Santiago, M.A., Ricker, M. and de Jong, B.H., 2010. Estimation of tropical forest structure from SPOT-5 satellite images. *International Journal of Remote Sensing*, 31, 2767-2782.
- Champion, I., Dubois-Fernandez, P., Guyon, D. and Cottrel, M., 2008. Radar image texture as a function of forest stand age. *International Journal of Remote Sensing*, 29, 1795-1800.
- Chen\*, D., Stow, D.A. and Gong, P., 2004. Examining the effect of spatial resolution and texture window size on classification accuracy: an urban environment case. *International Journal of Remote Sensing*, 25, 2177-2192.
- Cheng, P. and Chaapel, C., 2008. Increased image collection opportunities, Digital Globe's worldview-1 satellite. *Geoform. Online Mag.*
- Chetty, S. 2020. *Using spectral and textural information to detect and map Parthenium hysterophorus L. in Mtubatuba, South Africa.*
- Cho, M.A., Debba, P., Mathieu, R., Naidoo, L., Van Aardt, J.A.N. and Asner, G.P., 2010. Improving discrimination of savanna tree species through a multiple endmember spectral angle mapper approach: Canopy-level analysis. *IEEE Transactions on Geoscience and Remote Sensing*, 48, 4133-4142.
- Chun, H. and Keleş, S., 2010. Sparse partial least squares regression for simultaneous dimension reduction and variable selection. *Journal of the Royal Statistical Society: Series B (Statistical Methodology)*, 72, 3-25.
- Clarke, J. 2018. Job creation in agriculture, forestry and fisheries in South Africa: An analysis of employment trends, opportunities and constraints in forestry and wood products industries.
- DAFF 2008. Report on commercial timber resources and primary roundwood processing in South Africa 2006/7.
- DAFF. 2012. Report on commercial timber resources and primary roundwood processing in South Africa.

- Department of Agriculture, Forestry & Fisheries, Pretoria South Africa.
- Dube, T., Gara, T.W., Mutanga, O., Sibanda, M., Shoko, C., Murwira, A., Masocha, M., Ndaimani, H. and Hatendi, C.M., 2018. Estimating forest standing biomass in savanna woodlands as an indicator of forest productivity using the new generation WorldView-2 sensor. *Geocarto International*, 33, 178-188.
- Dube, T., Mutanga, O., Elhadi, A. and Ismail, R., 2014. Intra-and-inter species biomass prediction in a plantation forest: testing the utility of high spatial resolution spaceborne multispectral rapideye sensor and advanced machine learning algorithms. *Sensors*, 14, 15348-15370.
- Dube, T. and Mutanga, O., 2015. Investigating the robustness of the new Landsat-8 Operational Land Imager derived texture metrics in estimating plantation forest aboveground biomass in resource constrained areas. *ISPRS Journal of Photogrammetry and Remote sensing*, 108, 12-32.
- Dye, M., Mutanga, O. and Ismail, R., 2008. Detecting the severity of woodwasp, *Sirex noctilio*, infestation in a pine plantation in KwaZulu-Natal, South Africa, using texture measures calculated from high spatial resolution imagery. *African Entomology*, 16, 263-275.
- Dye, M., Mutanga, O. and Ismail, R., 2012. Combining spectral and textural remote sensing variables using random forests: predicting the age of *Pinus patula* forests in KwaZuluNatal, South Africa. *Journal of spatial science*, 57, 193-211.
- Eitel, J.U., Vierling, L.A., Litvak, M.E., Long, D.S., Schulthess, U., Ager, A.A., Krofcheck, D.J. and Stoscheck, L., 2011. Broadband, red-edge information from satellites improves early stress detection in a New Mexico conifer woodland. *Remote Sensing of Environment*, 115, 3640-3646.
- Fassnacht, F.E., Neumann, C., Förster, M., Buddenbaum, H., Ghosh, A., Clasen, A., Joshi, P.K. and Koch, B. 2014. Comparison of feature reduction algorithms for classifying tree species with hyperspectral data on three central European test sites. *IEEE Journal of Selected Topics in Applied Earth Observations and Remote Sensing*, 7, 2547-2561.
- Fassnacht, F.E., Neumann, C., Förster, M., Buddenbaum, H., Ghosh, A., Clasen, A., Joshi, P.K. and Koch, B., 2013. Spectral discrimination of giant reed (*Arundo donax* L.): A seasonal study in riparian areas. *ISPRS journal of photogrammetry and remote sensing*, 80, 80-90.
- Franklin, S.E., Hall, R.J., Moskal, L.M., Maudie, A.J. and Lavigne, M.B. 2000. Incorporating texture into classification of forest species composition from airborne multispectral images. *International journal of remote sensing*, 21, 61-79.
- Franklin, S.E., Wulder, M.A. and Lavigne, M.B., 1996. Automated derivation of geographic window sizes for use in remote sensing digital image texture analysis. *Computers & Geosciences*, 22, 665-673.
- Franklin, S. E. 2001. *Remote sensing for sustainable forest management*, CRC press.
- Fuchs, H., Magdon, P., Kleinn, C. and Flessa, H., 2009. Estimating aboveground carbon in a catchment of the Siberian forest tundra: Combining satellite imagery and field inventory. *Remote Sensing of Environment*, 113, 518-531.
- Galtier, O., Abbas, O., Le Dréau, Y., Rebufa, C., Kister, J., Artaud, J. & Dupuy, N. J. V. S. 2011. Comparison of PLS1-DA, PLS2-DA and SIMCA for classification by origin of crude petroleum oils by MIR and virgin olive oils by NIR for different spectral regions. *Vibrational Spectroscopy*, 55, 132-140.
- Gamon, J.A. and Surfus, J.S., 1999. Assessing leaf pigment content and activity with a reflectometer. *The New Phytologist*, 143, 105-117.
- Gebreslasie, M.T., Ahmed, F.B. and Van Aardt, J.A., 2011. Extracting structural attributes from IKONOS imagery for Eucalyptus plantation forests in KwaZulu-Natal, South Africa, using image texture analysis and artificial neural networks. *International journal of remote sensing*, 32, 7677-7701.
- Godsmark, R. and Oberholzer, F., 2008. The South African forestry and forest products industry 2007.
- Gómez, W., Pereira, W.C.A. and Infantosi, A.F.C., 2012. Analysis of cooccurrence texture statistics as a function of gray-level quantization for classifying breast ultrasound. *IEEE transactions on medical imaging*, 31, 1889-1899.

- Gong, P., Pu, R., Biging, G.S. and Larrieu, M.R. 2003. Estimation of forest leaf area index using vegetation indices derived from Hyperion hyperspectral data. *IEEE transactions on geoscience and remote sensing*, 41, 1355-1362.
- Gwata, B. Developing high resolution clutter for wireless network propagation using WorldView-2 imagery. Algorithms and Technologies for Multispectral, Hyperspectral, and Ultraspectral Imagery XVIII, 2012. *International Society for Optics and Photonics*, 83902Q.
- Haboudane, D., Miller, J.R., Pattey, E., Zarco-Tejada, P.J. and Strachan, I.B., 2004. Hyperspectral vegetation indices and novel algorithms for predicting green LAI of crop canopies: Modeling and validation in the context of precision agriculture. *Remote sensing of environment*, 90, 337-352.
- Haralick, R.M., Shanmugam, K. and Dinstein, I.H., 1973. Textural features for image classification. *IEEE Transactions on systems, man, and cybernetics*, 610-621.
- Hlatshwayo, S.T., Mutanga, O., Lottering, R.T., Kiala, Z. and Ismail, R., 2019. Mapping forest aboveground biomass in the reforested Buffelsdraai landfill site using texture combinations computed from SPOT-6 pan-sharpened imagery. *Journal of Applied Earth Observation and Geoinformation*, 74, 65-77.
- Huete, A., Didan, K., Miura, T., Rodriguez, E.P., Gao, X. and Ferreira, L.G., 2002. Overview of the radiometric and biophysical performance of the MODIS vegetation indices. *Remote sensing of environment*, 83, 195-213.
- Ingram, J.C., Dawson, T.P. and Whittaker, R.J., 2005. Mapping tropical forest structure in southeastern Madagascar using remote sensing and artificial neural networks. *Remote Sensing of Environment*, 94, 491-507.
- Ismail, R., Mutanga, O. and Ahmed, F., 2008. Discriminating Sirex noctilio attack in pine forest plantations in South Africa using high spectral resolution data. In *Hyperspectral remote sensing of tropical and subtropical forests* 161-174.
- Kaufman, Y.J. and Tanre, D., 1996. Strategy for direct and indirect methods for correcting the aerosol effect on remote sensing: from AVHRR to EOS-MODIS. *Remote sensing of Environment*, 55, 65-79.
- Kpalma, K., El-Mezouar, M.C. and Taleb, N., 2014. Recent trends in satellite image pan-sharpening techniques. In *1st International Conference on Electrical, Electronic and Computing Engineering*.
- Lê Cao, K.A., Rossouw, D., Robert-Granié, C. and Besse, P., 2008. A sparse PLS for variable selection when integrating omics data. *Statistical applications in genetics and molecular biology*, 7.
- Li, J., Rich, W. and Buhl-Brown, D., 2015. Texture analysis of remote sensing imagery with clustering and Bayesian inference. *Int. J. Image Graph. Sig. Proces. (IJIGSP)*, 7, 1-10.
- Li, L., Cheng, Y.B., Ustin, S., Hu, X.T. and Riaño, D., 2008. Retrieval of vegetation equivalent water thickness from reflectance using genetic algorithm (GA)-partial least squares (PLS) regression. *Advances in Space Research*, 41, 1755-1763.
- Li, L., Ustin, S.L. and Riano, D., 2007. Retrieval of fresh leaf fuel moisture content using genetic algorithm partial least squares (GA-PLS) modeling. *IEEE Geoscience and Remote Sensing Letters*, 4, 216-220.
- Lottering, R., Mutanga, O., Peerbhay, K. and Ismail, R., 2019. Detecting and mapping Gonipterus scutellatus induced vegetation defoliation using WorldView-2 pansharpened image texture combinations and an artificial neural network. *Journal of Applied Remote Sensing*, 13, 014513.
- Lottering, R., Mutanga, O. and Peerbhay, K., 2018. Detecting and mapping levels of Gonipterus scutellatus-induced vegetation defoliation and leaf area index using spatially optimized vegetation indices. *Geocarto international*, 33, 277-292.



- Lottering, R. and Mutanga, O., 2016. Optimising the spatial resolution of WorldView-2 pan-sharpened imagery for predicting levels of *Gonipterus scutellatus* defoliation in KwaZulu-Natal, South Africa. *ISPRS journal of photogrammetry and remote sensing*, 112, 13-22.
- Lottering, R. and Mutanga, O., 2012. Estimating the road edge effect on adjacent *Eucalyptus grandis* forests in KwaZulu-Natal, South Africa, using texture measures and an artificial neural network. *Journal of Spatial Science*, 57, 153-173.
- Lottering, R.T., Govender, M., Peerbhay, K. and Lottering, S., 2020. Comparing partial least squares (PLS) discriminant analysis and sparse PLS discriminant analysis in detecting and mapping *Solanum mauritianum* in commercial forest plantations using image texture. *ISPRS Journal of Photogrammetry and Remote Sensing*, 159, 271-280.
- Lu, D. and Batistella, M., 2005. Exploring TM image texture and its relationships with biomass estimation in Rondônia, Brazilian Amazon. *Acta Amazonica*, 35, 249-257.
- Lu, D., Mausel, P., Brondizio, E. and Moran, E., 2002. Above-ground biomass estimation of successional and mature forests using TM images in the Amazon Basin. *Advances in spatial data handling*. Springer.
- Lu, D., 2006. The potential and challenge of remote sensing-based biomass estimation. *International journal of remote sensing*, 27, 1297-1328.
- Maccioni, A., Agati, G. and Mazzinghi, P., 2001. New vegetation indices for remote measurement of chlorophylls based on leaf directional reflectance spectra. *Journal of Photochemistry and Photobiology B: Biology*, 61, 52-61.
- Marceau, D.J., Howarth, P.J., Dubois, J.M.M. and Gratton, D.J., 1990. Evaluation of the grey-level co-occurrence matrix method for land-cover classification using SPOT imagery. *IEEE Transactions on Geoscience and Remote Sensing*, 28, 513-519.
- Materka, A. and Strzelecki, M., 1998. Texture analysis methods—a review. *Technical university of lodz, institute of electronics*, 10, 4968.
- Mather, P. M. & Koch, M. 2011. *Computer processing of remotely-sensed images: an introduction*, John Wiley & Sons.
- Menze, B.H., Kelm, B.M., Masuch, R., Himmelreich, U., Bachert, P., Petrich, W. and Hamprecht, F.A., 2009. A comparison of random forest and its Gini importance with standard chemometric methods for the feature selection and classification of spectral data. *BMC bioinformatics*, 10, 213.
- Menze, B.H., Kelm, B.M., Masuch, R., Himmelreich, U., Bachert, P., Petrich, W. and Hamprecht, F.A., 2019. Examining the effectiveness of Sentinel-1 and 2 imagery for commercial forest species mapping. *Geocarto International*, 1-12.
- Moskal, L.M. and Franklin, S.E., 2004. Relationship between airborne multispectral image texture and aspen defoliation. *International journal of remote sensing*, 25, 2701-2711.
- Mushore, T.D., Mutanga, O., Odindi, J. and Dube, T., 2017. Assessing the potential of integrated Landsat 8 thermal bands, with the traditional reflective bands and derived vegetation indices in classifying urban landscapes. *Geocarto international*, 32, 886-899.
- Mutanga, O., Adam, E. and Cho, M.A., 2012. High density biomass estimation for wetland vegetation using WorldView-2 imagery and random forest regression algorithm. *International Journal of Applied Earth Observation and Geoinformation*, 18, 399-406.
- Mutanga, O. and Skidmore, A.K., 2004. Narrow band vegetation indices overcome the saturation problem in biomass estimation. *International journal of remote sensing*, 25(19), 25, 3999-4014.
- Myneni, R.B., Hall, F.G., Sellers, P.J. and Marshak, A.L., 1995. The interpretation of spectral vegetation indexes. *IEEE Transactions on Geoscience and Remote Sensing*, 33, 481-486.
- Nichol, J.E. and Sarker, M.L.R., 2010. Improved biomass estimation using the texture parameters of two high-resolution optical sensors. *IEEE Transactions on Geoscience and Remote Sensing*, 49, 930-948.

- Omar, H., 2010. Commercial timber tree species identification using multispectral Worldview2 data. *Digital Globe® 8Bands Research Challenge*, 2-13.
- Peerbhay, K.Y., Mutanga, O. and Ismail, R., 2013a. Commercial tree species discrimination using airborne AISA Eagle hyperspectral imagery and partial least squares discriminant analysis (PLS-DA) in KwaZulu-Natal, South Africa. *ISPRS Journal of Photogrammetry and Remote Sensing*, 79, 19-28.
- Peerbhay, K.Y., Mutanga, O. and Ismail, R., 2013b. Investigating the capability of few strategically placed Worldview-2 multispectral bands to discriminate forest species in KwaZulu-Natal, South Africa. *IEEE Journal of Selected Topics in Applied Earth Observations and Remote Sensing*, 7, 307-316.
- Peerbhay, K.Y., Mutanga, O. and Ismail, R., 2014. Does simultaneous variable selection and dimension reduction improve the classification of Pinus forest species? *Journal of Applied Remote Sensing*, 8(1), p.085194. 8, 085194.
- Rao, P.N., Sai, M.S., Sreenivas, K., Rao, M.K., Rao, B.R.M., Dwivedi, R.S. and Venkataratnam, L., 2002. Textural analysis of IRS-1D panchromatic data for land cover classification. *International Journal of Remote Sensing*, 23, 3327-3345.
- Puzicha, J., Buhmann, J.M., Rubner, Y. and Tomasi, C., 2001. Empirical evaluation of dissimilarity measures for color and texture. *Computer vision and image understanding*, 84, 25-43.
- Salas, E.A.L., Boykin, K.G. and Valdez, R., 2016. Multispectral and texture feature application in image-object analysis of summer vegetation in Eastern Tajikistan Pamirs. *Remote Sensing*, 8, 78.
- Sarker, L.R. and Nichol, J.E., 2011. Improved forest biomass estimates using ALOS AVNIR-2 texture indices. *Remote Sensing of Environment*, 115, 968-977.
- Sesnie, S.E., Finegan, B., Gessler, P.E., Thessler, S., Ramos Bendana, Z. and Smith, A.M., 2010. The multispectral separability of Costa Rican rainforest types with support vector machines and Random Forest decision trees. *International Journal of Remote Sensing*, 31, 2885-2909.
- Sibanda, M., Mutanga, O., Rouget, M. and Odindi, J., 2015. Exploring the potential of in situ hyperspectral data and multivariate techniques in discriminating different fertilizer treatments in grasslands. *Journal of Applied Remote Sensing*, 9, 096033.
- Sims, D.A. and Gamon, J.A., 2002. Relationships between leaf pigment content and spectral reflectance across a wide range of species, leaf structures and developmental stages. *Remote sensing of environment*, 81, 337-354.
- Sripada, R.P., Heiniger, R.W., White, J.G. and Meijer, A.D., 2006. Aerial color infrared photography for determining early in-season nitrogen requirements in corn. *Agronomy Journal*, 98, 968-977.
- St-Louis, V., Pidgeon, A.M., Radeloff, V.C., Hawbaker, T.J. and Clayton, M.K., 2006. High-resolution image texture as a predictor of bird species richness. *Remote Sensing of Environment*, 105, 299-312.
- Team, R. C. 2013. R: A language and environment for statistical computing. Vienna, Austria.
- Van Aardt, J.A.N. and Wynne, R.H., 2007. Examining pine spectral separability using hyperspectral data from an airborne sensor: An extension of field-based results. *International Journal of Remote Sensing*, 28, 431-436.
- Wang, W., Yao, X., Yao, X., Tian, Y., Liu, X., Ni, J., Cao, W. and Zhu, Y., 2012. Estimating leaf nitrogen concentration with three-band vegetation indices in rice and wheat. *Field Crops Research*, 129, 90-98.
- Wolter, P.T., Townsend, P.A., Sturtevant, B.R. and Kingdon, C.C., 2008. Remote sensing of the distribution and abundance of host species for spruce budworm in Northern Minnesota and Ontario. *Remote Sensing of Environment*, 112, 3971-3982.

- Yu, Q., Gong, P., Clinton, N., Biging, G., Kelly, M. and Schirokauer, D., 2006. Object-based detailed vegetation classification with airborne high spatial resolution remote sensing imagery. *Photogrammetric Engineering & Remote Sensing*, 72, 799-811.
- Yuan, X., King, D. and Vlcek, J., 1991. Sugar maple decline assessment based on spectral and textural analysis of multispectral aerial videography. *Remote Sensing of Environment*, 37, 47-54.